Article

Developmental Cell

Extracellular carriers control lipid-dependent secretion, delivery, and activity of WNT morphogens

Graphical abstract

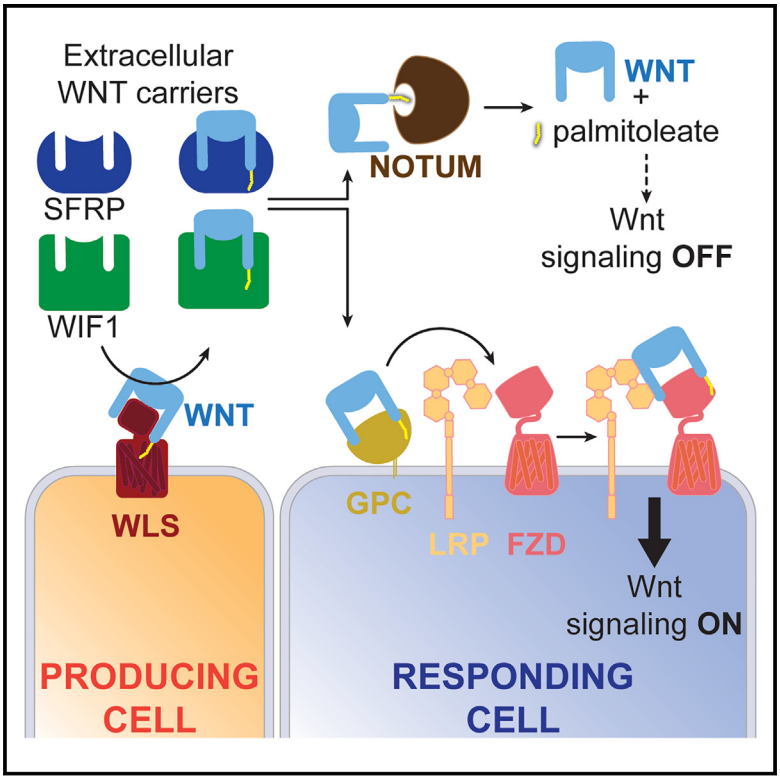

Highlights

- Lipid-modified WNTs are released from cells in complex with SFRP and WIF1 carriers
- WNT carrier complexes are soluble and active in signaling
- WNT transfer from carriers to FZD receptors is facilitated by glypican co-receptors
- Some carriers transfer WNTs to the WNT-antagonizing lipid hydrolase NOTUM

Authors

Taciani de Almeida Magalhaes, Jingjing Liu, Charlene Chan, ..., David T. Breault, Pengxiang Huang, Adrian Salic

Correspondence

taciani_magalhaes@hms.harvard.edu (T.d.A.M.), asalic@hms.harvard.edu (A.S.)

In brief

de Almeida Magalhaes et al. demonstrate that lipidated WNT morphogens are secreted by handoff from the membrane protein WLS to extracellular carrier proteins. Soluble WNT carrier complexes deliver WNTs to target cells or the inhibitory NOTUM hydrolase. These mechanisms explain how WNTs spread extracellularly to activate signaling in faraway cells.

de Almeida Magalhaes et al., 2024, Developmental Cell *59*, 1–18
January 22, 2024
https://doi.org/10.1016/j.devcel.2023.11.027

CellPress

Please cite this article in press as: de Almeida Magalhaes et al., Extracellular carriers control lipid-dependent secretion, delivery, and activity of WNT morphogens, Developmental Cell (2023), https://doi.org/10.1016/j.devcel.2023.11.027

Developmental Cell

CellPress

Article

Extracellular carriers control lipid-dependent secretion, delivery, and activity of WNT morphogens

Taciani de Almeida Magalhaes,[1,7,*] Jingjing Liu,[1,7] Charlene Chan,[1] Kleiton Silva Borges,[2,3] Jiuchun Zhang,[1] Andrew J. Kane,[4] Bradley M. Wierbowski,[1] Yunhui Ge,[5] Zhiwen Liu,[5] Prabhath Mannam,[2] Daniel Zeve,[2,3] Ron Weiss,[4] David T. Breault,[2,3,6] Pengxiang Huang,[5] and Adrian Salic[1,8,*]

[1]Department of Cell Biology, Blavatnik Institute, Harvard Medical School, Boston, MA 02115, USA
[2]Division of Endocrinology, Boston Children's Hospital, Boston, MA 02115, USA
[3]Department of Pediatrics, Harvard Medical School, Boston, MA 02115, USA
[4]Synthetic Biology Center, Massachusetts Institute of Technology, Cambridge, MA 02139, USA
[5]Department of Molecular and Cellular Biology, Baylor College of Medicine, Houston, TX 77030, USA
[6]Harvard Stem Cell Institute, 7 Divinity Avenue, Cambridge, MA 02138, USA
[7]These authors contributed equally
[8]Lead contact
*Correspondence: taciani_magalhaes@hms.harvard.edu (T.d.A.M.), asalic@hms.harvard.edu (A.S.)
https://doi.org/10.1016/j.devcel.2023.11.027

SUMMARY

WNT morphogens trigger signaling pathways fundamental for embryogenesis, regeneration, and cancer. WNTs are modified with palmitoleate, which is critical for binding Frizzled (FZD) receptors and activating signaling. However, it is unknown how WNTs are released and spread from cells, given their strong lipid-dependent membrane attachment. We demonstrate that secreted FZD-related proteins and WNT inhibitory factor 1 are WNT carriers, potently releasing lipidated WNTs and forming active soluble complexes. WNT release occurs by direct handoff from the membrane protein WNTLESS to the carriers. In turn, carriers donate WNTs to glypicans and FZDs involved in WNT reception and to the NOTUM hydrolase, which antagonizes WNTs by lipid moiety removal. WNT transfer from carriers to FZDs is greatly facilitated by glypicans that serve as essential co-receptors in Wnt signaling. Thus, an extracellular network of carriers dynamically controls secretion, posttranslational regulation, and delivery of WNT morphogens, with important practical implications for regenerative medicine.

INTRODUCTION

Morphogens are secreted proteins that spread from producing cells and activate signaling pathways that control the fate of distant cells.[1] Morphogens of the WNT family, which has 19 members in humans, are critical for numerous developmental processes,[2] post-embryonic regeneration,[3,4] and tissue homoeostasis.[4,5] Deficient Wnt signaling during development causes birth defects,[6] whereas excessive signaling is involved in multiple cancers.[3,7,8]

WNTs signal by engaging a receptor of the GPCR-related Frizzled (FZD) family[9] and a co-receptor. Depending on the co-receptor employed, WNTs elicit distinct downstream transduction cascades.[10] Canonical WNTs (such as WNT3A) use the lipoprotein-receptor-related proteins LRP5 and LRP6 as co-receptors[11,12] and stabilize the transcriptional co-activator β-catenin, thus eliciting a specific transcriptional program.[13,14] Non-canonical WNTs (such as WNT5A) utilize the tyrosine-kinase-like orphan receptors ROR1 and ROR2 as co-receptors[15,16] and exert effects on cell and tissue polarity via transcription-independent mechanisms involving c-Jun N-terminal kinase (JNK) or Ca^{2+} signaling.[17,18]

All WNTs are modified with palmitoleic acid on a conserved serine residue,[19,20] catalyzed by the endoplasmic reticulum (ER)-resident O-acyl-transferase, Porcupine (PORCN).[21,22] Lipidation plays a key role in several steps in Wnt signaling. First, it is required for WNT secretion, by interaction with the essential membrane protein WNTLESS (WLS),[23,24] which escorts WNTs from the ER to the cell surface. Second, in *Drosophila*, WNTs interact in a lipid-dependent manner with the glypican Dally-like protein (Dlp),[25] a GPI-anchored proteoglycan required for Wnt signaling upstream of FZD. Third, lipidation is critical for WNT binding to FZDs[9] and thus for initiating signaling.

Lipidated WNTs are also regulated by several extracellular proteins. The acyl-hydrolase NOTUM interacts with WNTs and removes their palmitoleate moiety,[26] thus inactivating them. In vertebrates, two developmentally expressed classes of proteins, the secreted FZD-related protein (SFRP) family[27,28] and WNT inhibitory factor 1 (WIF1),[29] bind WNTs in a lipid-dependent manner[30,31]

Please cite this article in press as: de Almeida Magalhaes et al., Extracellular carriers control lipid-dependent secretion, delivery, and activity of WNT morphogens, Developmental Cell (2023), https://doi.org/10.1016/j.devcel.2023.11.027

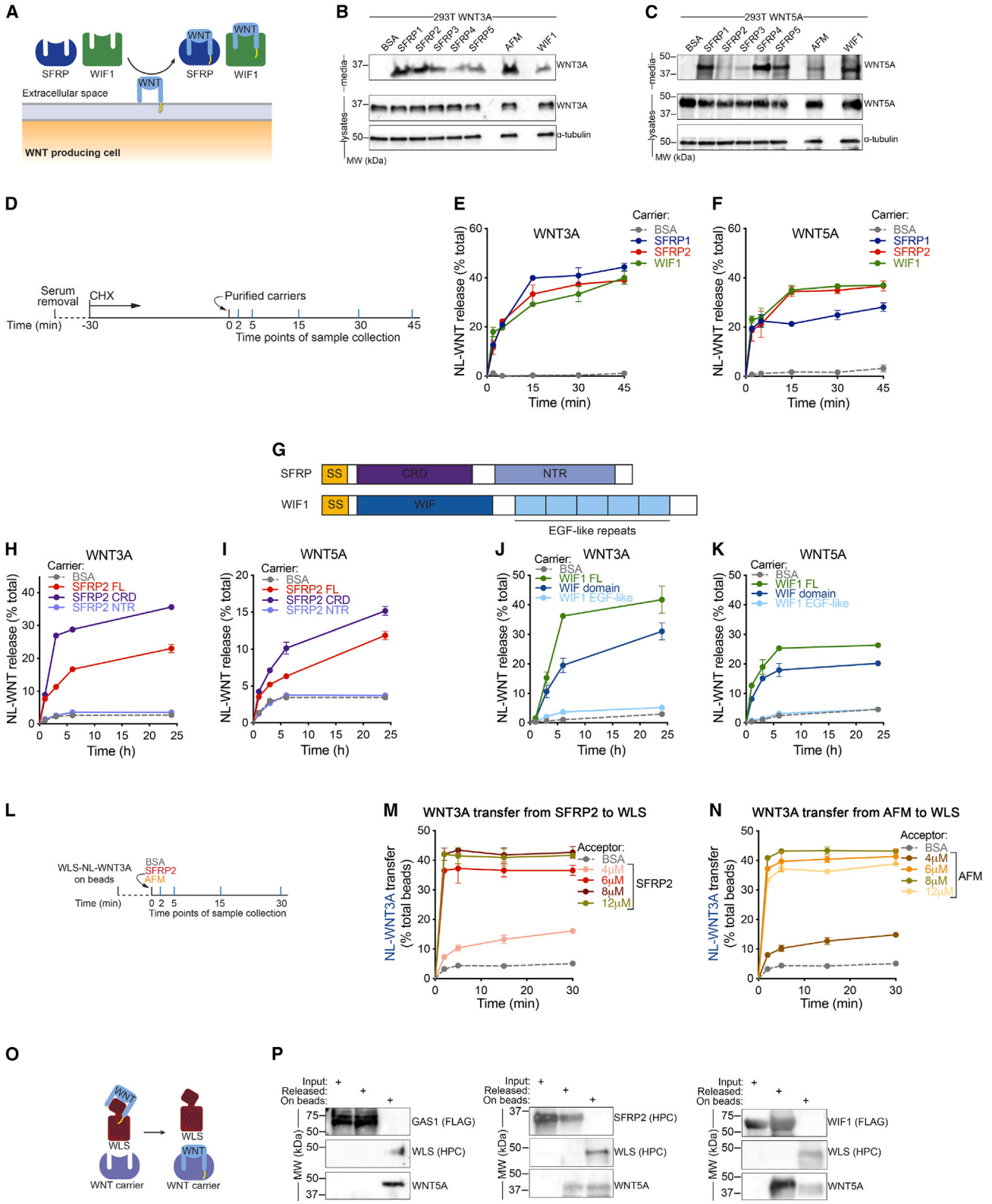

Figure 1. SFRPs and WIF1 rapidly release WNTs from cells by direct handoff from WLS

(A) Model of WNT release from cells by SFRPs and WIF1.

(B) Purified SFRPs and WIF1 (1 μM) were added to WNT3A-producing cells, and WNT released into serum-free media was assayed by immunoblotting. Incubation with bovine serum albumin (BSA) and AFM served as negative and positive control, respectively. See Figure S1A for protein purification.

(legend continued on next page)

Please cite this article in press as: de Almeida Magalhaes et al., Extracellular carriers control lipid-dependent secretion, delivery, and activity of WNT morphogens, Developmental Cell (2023), https://doi.org/10.1016/j.devcel.2023.11.027

and are thought to inhibit signaling,[29–32] by competing for the interaction with FZD.

Although essential for function, lipid modification renders WNTs highly hydrophobic and thus strongly attached to membranes,[33] a property that has long frustrated efforts to obtain active soluble WNTs. Currently, purified WNTs are kept soluble using detergent, but such preparations have poor stability.[34,35] Aqueous insolubility of WNTs also raises the fundamental question of how they spread from producing cells to signal at a distance. Over the years, various models have been proposed to account for long-range WNT transport. In one class of models, WNTs are transported by particulate carriers, such as exosomes[36,37] and lipoproteins.[38] Recently, however, experiments in *Drosophila*[26] showed that neither exosomes nor lipoproteins are required for Wnt signaling and failed to detect an interaction between these particles and Wingless (Wg), the major WNT ligand in flies. In another model, WNTs are transported on the surface of actin-based protrusions that emanate from WNT-producing cells, called cytonemes.[39] Although cytonemes could explain the spread of WNTs, the question remains of how WNTs are solubilized, to move from the cytoneme membrane to the target cell. However, another category of models involves dedicated WNT carriers. This was first suggested by the observation that serum releases WNTs from cultured cells,[40] an activity later ascribed to Afamin (AFM),[41] a serum albumin protein family member. However, Wnt signaling begins in early development, well before fetal circulation, leaving open the question of how WNTs are released during this period. Furthermore, it is unclear whether AFM requires WLS for WNT solubilization or if AFM and WLS operate in distinct pathways. Finally, carriers are expected to interact with the WNT lipid moiety, which is critical for binding to FZDs, raising the question of how WNTs can be exchanged between mutually exclusive partners.

Here, we investigate the mechanisms by which vertebrate WNTs are solubilized and delivered to responding cells. We show that SFRPs and WIF1 are WNT carriers, rapidly releasing WNTs from cells in a lipid- and WLS-dependent manner. We demonstrate that WNT release occurs by direct handoff from WLS to carriers. WNT release by AFM also requires WLS, indicating that WLS can donate WNTs to diverse carriers. Strikingly, the soluble and highly stable WNT carrier complexes activate Wnt signaling, in contrast with the long-standing idea that SFRPs and WIF1 are inhibitory, a behavior observed at high carrier excess. WNT carrier complexes can transfer WNTs directly to FZDs, but the process is greatly facilitated by a subset of vertebrate glypicans (GPCs), providing a mechanism for the essential role we find for GPCs in vertebrate Wnt signaling. The carriers can also hand off WNTs to NOTUM, thus facilitating WNT inactivation. Finally, we uncover evidence of specificity in the transfer of WNTs from carriers to NOTUM. Our results define a complex network of extracellular lipid-dependent carriers that control the spreading and activity of WNT morphogens and define strategies for producing active and stable WNT preparations for regenerative medicine.

RESULTS

SFRPs and WIF1 promote the release of WNTs from cells

We hypothesized that dedicated carriers solubilize WNTs during embryogenesis, by shielding the palmitoleate moiety (Figure 1A). We thus tested whether WNTs can be released from cells by two developmentally expressed protein families implicated in binding lipidated WNTs: SFRPs,[27,43] which include five members in humans, and WIF1, with one member.[29] As shown in Figures 1B and 1C, both canonical WNT3A and non-canonical WNT5A were not secreted in the absence of serum. Adding purified SFRPs 1–5 or WIF1 (Figure S1A) caused robust secretion of

(C) As in (B), but with WNT5A-producing cells.
(D) Schematic of the NanoLuc luciferase (NL) WNT release assay. Cells stably expressing NL-WNT are pre-incubated with cycloheximide (CHX) to inhibit protein synthesis. NL-WNT release is initiated by addition of carrier (1 μM) in serum-free media and is measured at various time points by NL luminescence.
(E) Kinetics of NL-WNT3A release by purified carriers (1 μM), measured as in (D). Data represent the mean of two biological and three technical replicates, normalized to total NL-WNT in lysates, and error bars show SD. See Figures S1B–S1L and S2A–S2D for additional characterization of WNT release and its dependence on PORCN and WLS.
(F) As in (E), but measuring NL-WNT5A release.
(G) Domain structure of SFRPs and WIF1.
(H) NL-WNT3A release by purified full-length (FL) SFRP2, CRD only, or NTR domain only (1 μM each). BSA was used as negative control. CRD is necessary and sufficient for WNT release. Data represent the mean of two biological and three technical replicates, normalized by total NL activity in the lysates, and error bars show SD. See Figure S1H for protein purification.
(I) As in (H), but measuring NL-WNT5A release.
(J) As in (H), but with purified FL WIF1, WIF domain only, or WIF1 EGF-like domains only (1 μM). WIF domain is necessary and sufficient for WNT3A release. See Figure S1I for protein purification.
(K) As in (J), but measuring NL-WNT5A release.
(L) Experimental setup for WNT transfer from WLS-NL-WNT beads to carriers.
(M) WLS-NL-WNT3A complex was covalently captured on HaloLink beads, via HaloTag (HT7) attached to the C terminus of WLS. The beads were then incubated with SFRP2 (4, 6, 8, and 12 μM), and NL-WNT release was measured at various time points. Incubation with BSA (12 μM) served as negative control. NL-WNT3A is rapidly transferred from WLS to SFRP2, reaching saturation at 6 μM. Points represent average of two biological and three technical replicates, normalized to total NL-WNT on beads, and error bars represent SD.
(N) As in (M), but WLS-NL-WNT3A beads were incubated with AFM (4, 6, 8, and 12 μM).
(O) Schematic for WNT transfer from WLS to carriers.
(P) WLS-WNT5A complex was captured on antibody beads via a HPC tag attached to the C terminus of WLS. The beads were incubated with SFRP2 or WIF1 (3 μM), and WNT5A release was measured by immunoblotting. Incubation with the ectodomain of GAS1[42] served as negative control. WNT5A is transferred to SFRP2 and WIF1, but not to GAS1. See Figures S2E and S2F for WLS-WNT5A purification.
See also Figures S1 and S2 for additional characterization of carrier purification, NL-WNTs release, and role of PORCN and WLS in WNT release by carriers.

Please cite this article in press as: de Almeida Magalhaes et al., Extracellular carriers control lipid-dependent secretion, delivery, and activity of WNT morphogens, Developmental Cell (2023), https://doi.org/10.1016/j.devcel.2023.11.027

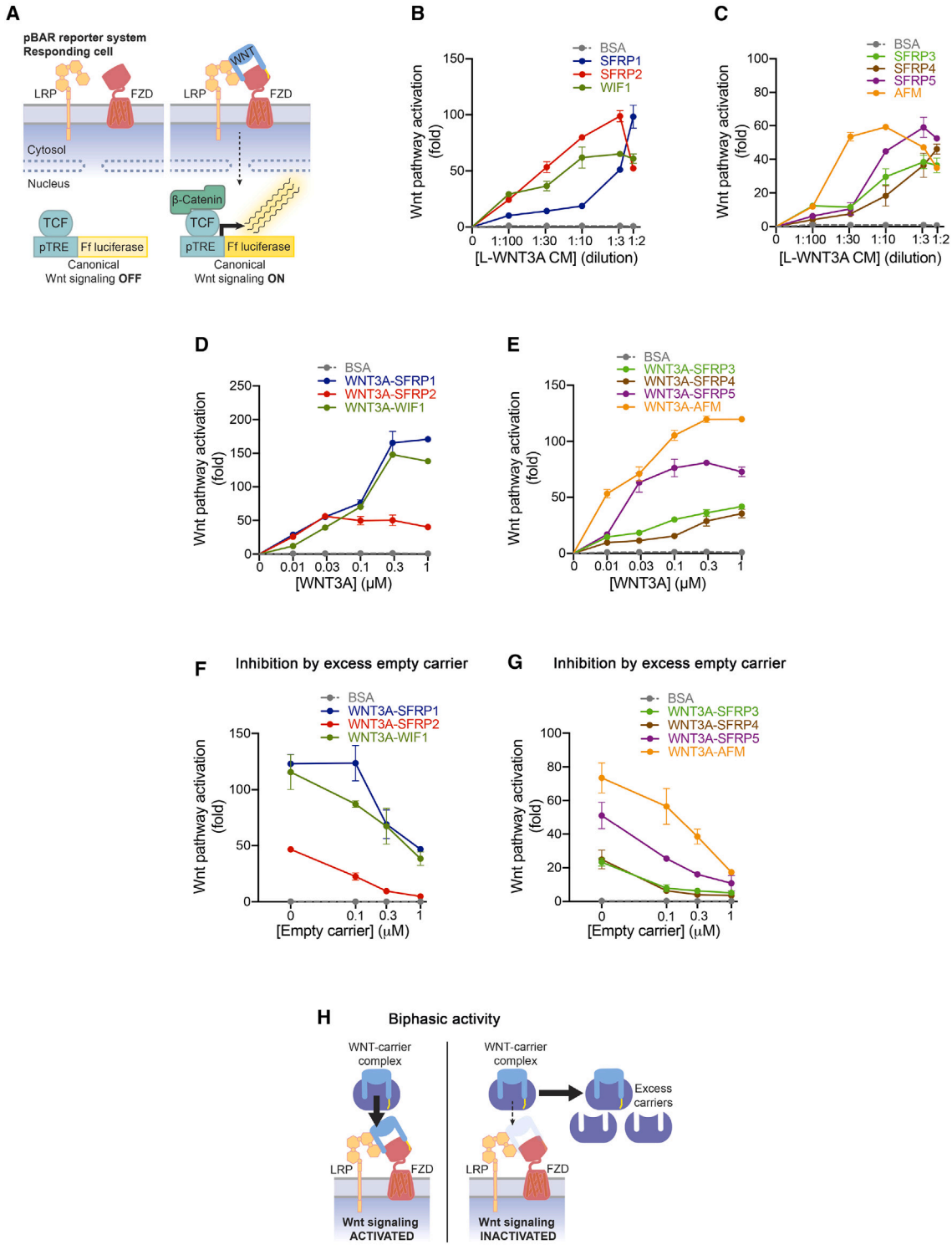

Figure 2. WNT3A-carrier complexes activate Wnt signaling

(A) Schematic of canonical Wnt reporter system, consisting of firefly (Ff) luciferase under the control of a TCF-responsive promoter (pTRE)[45,46] and constitutively expressed Renilla luciferase. Left: in the absence of stimulation, TCF proteins repress transcription. Right: upon Wnt stimulation, β-catenin accumulates and forms a complex with TCF that activates target gene expression.

(B) Purified carriers (1 μM) were added to L-WNT3A cells and Wnt activity was measured in serial dilutions of the conditioned media. Incubation with BSA served as negative control. WNT3A released by SFRP1, SFRP2, and WIF1 activates signaling. Points represent average activation for two biological and three technical

(legend continued on next page)

Please cite this article in press as: de Almeida Magalhaes et al., Extracellular carriers control lipid-dependent secretion, delivery, and activity of WNT morphogens, Developmental Cell (2023), https://doi.org/10.1016/j.devcel.2023.11.027

WNT3A and WNT5A, similar to the serum carrier, AFM[41] (Figures 1B and 1C). These results indicate that all SFRPs and WIF1 can release WNTs from cells.

To characterize WNT release with greater sensitivity and temporal resolution, we turned to WNTs tagged with NanoLuc luciferase (NL)[44] (Figure S1B). As shown in Figures S1C–S1E, various NL-tagged WNTs were readily released by SFRPs and WIF1 but not by serum-free media, indicating that NL-WNTs recapitulate the behavior of untagged WNTs. To determine secretion kinetics without the confounding effect of continued synthesis, we measured NL-WNT release from cells in which translation was blocked (Figure 1D). Under these conditions, WNT release by SFRPs and WIF1 was observed after as little as 2 min, continuing linearly and reaching a plateau after 15–30 min (Figures 1E, 1F, S1F, and S1G). These data indicate that WNT release by carriers is rapid and saturable, consistent with a binding equilibrium between WNTs and their carriers.

Finally, we asked if WNT release involves the carriers' lipid-binding domains, represented by the cysteine-rich domain (CRD)[9] of SFRPs and the WIF domain[31] of WIF1. To this end, we purified separately the CRD and the netrin-related motif (NTR) of SFRP2 and the WIF domain and epidermal growth factor (EGF)-like domains (WIF1 EGF-like) of WIF1 (Figures 1G, S1H, and S1I). WNTs were released by SFRP2-CRD but not by SFRP2-NTR (Figures 1H and 1I) and the WIF domain, but not by WIF1 EGF-like (Figures 1J and 1K). Thus, the lipid-binding domains of the carriers are necessary and sufficient for WNT release, suggesting that carriers solubilize WNTs by shielding their lipid moiety.

WNT release by SFRPs and WIF1 is lipid and WLS dependent

PORCN[21,22] and WLS[23,24] are essential for WNT biosynthesis, by catalyzing lipid modification and transporting WNTs to the plasma membrane, respectively. We thus asked whether PORCN and WLS are required for WNT release by carriers. Pharmacological inhibition of PORCN potently blocked WNT release by all carriers (Figures S1J–S1L). Similarly, WNT release was abolished (Figures S2A–S2D) in WLS^{KO} cells (Table S1), which was reversed by reintroducing WLS (Figures S2A–S2D). Together, these results indicate that WNT release by all carriers requires WNT lipidation and WLS.

WNTs are directly handed off from WLS to carriers

The movement of WNTs from WLS to carriers might occur by direct handoff or indirectly, via an intermediate. To distinguish between these possibilities, we assayed the transfer of NL-WNT3A from WLS on beads to purified SFRP2 and AFM in solution (Figure 1L). As shown in Figures 1M and 1N, NL-WNT3A was rapidly transferred to SFRP2 and AFM, but not to a control protein; importantly, the transfer was dose dependent and saturable by carrier. Furthermore, a purified stoichiometric WLS-WNT5A complex (Figures S2E and S2F) readily transferred WNT5A to SFRP2 and WIF1 (Figures 1O and 1P). These results demonstrate that lipidated WNTs are directly discharged from WLS to carriers. They also show that WLS, which is broadly required for WNT secretion, can interface with several unrelated extracellular carriers.

WNT3A carrier complexes activate signaling

We first asked whether WNT3A released by carriers can activate canonical Wnt signaling[45,46] (Figure 2A). Strikingly, WNT3A released by all SFRPs and WIF1 robustly activated Wnt signaling in a dose-dependent and saturable manner, similar to WNT3A released by AFM (Figures 2B, 2C, S3A, and S3B). Consistent with our release results, PORCN inhibition or WLS loss extinguished the signaling activity of conditioned media from WNT3A-expressing cells incubated with carriers (Figures S3C and S3D). These data demonstrate that all carriers promote the release of lipidated, active WNT3A.

The experiments above were performed using conditioned media, allowing the possibility that other factors might affect Wnt signaling in responding cells. To directly test the activity of WNT3A carrier complexes, we affinity-purified them using a tag attached to carriers. As shown in Figures S3E and S3F, WNT3A co-purified with SFRPs and WIF1, suggesting that they form stable complexes. Based on Coomassie blue staining and quantitative immunoblotting (Figures S3G–S3J), the WNT3A carrier preparations appear sub-stoichiometric with respect to WNT3A, likely because of limiting WNT3A expression. We did not attempt to obtain stoichiometric complexes by tandem affinity purification, as tagging WNT3A resulted in a severe loss of activity in our hands. Even so, sub-stoichiometric WNT3A carrier complexes strongly activated Wnt signaling (Figures 2D and 2E). These results indicate that WNT3A forms active water-soluble complexes with all SFRPs and WIF1.

Excess carriers antagonize signaling by WNT3A-carrier complexes

Activity of WNT3A carrier complexes was surprising, given numerous reports of the inhibitory role of SFRPs and WIF1 in Wnt signaling (for example, Hsieh et al.,[29] Dann et al.,[30]

replicates, normalized to untreated reporter cells, and error bars represent SD. See Figures S3A–S3D for the activity of WNT3A released by carriers from HEK293 cells, and the dependence of WNT3A release and activity on PORCN and WLS.

(C) As in (B), but with purified SFRP3, SFRP4, SFRP5, and AFM (1 μM).

(D) As in (B), but with a dose-response for purified WNT3A-SFRP1, WNT3A-SFRP2, and WNT3A-WIF1 (0.01, 0.03, 0.1, 0.3, and 1 μM with respect to WNT3A). See also Figures S3E–S3J for complex purification, quantitative immunoblotting, and standard WNT3A curves.

(E) As in (D), but with purified WNT3A-SFRP3, WNT3A-SFRP4, WNT3A-SFRP5, and WNT3A-AFM complexes (0.01, 0.03, 0.1, 0.3, and 1 μM with respect to WNT3A).

(F) As in (D), but with WNT3A-SFRP1, WNT3A-SFRP2, and WNT3A-WIF1 complexes (1 μM) supplemented with additional carrier. Excess carrier inhibits WNT3A activity in a dose-dependent manner.

(G) As in (F), but with purified WNT3A-SFRP3, WNT3A-SFRP4, WNT3A-SFRP5, and WNT3A-AFM (1 μM).

(H) Model for biphasic activity of carriers. Soluble WNT carrier complexes activate the Wnt pathway (left). High carrier concentrations compete with FZDs for binding to WNTs, leading to inhibition (right).

See also Figure S3 for additional characterization of the signaling activity of WNT3A-carriers.

Please cite this article in press as: de Almeida Magalhaes et al., Extracellular carriers control lipid-dependent secretion, delivery, and activity of WNT morphogens, Developmental Cell (2023), https://doi.org/10.1016/j.devcel.2023.11.027

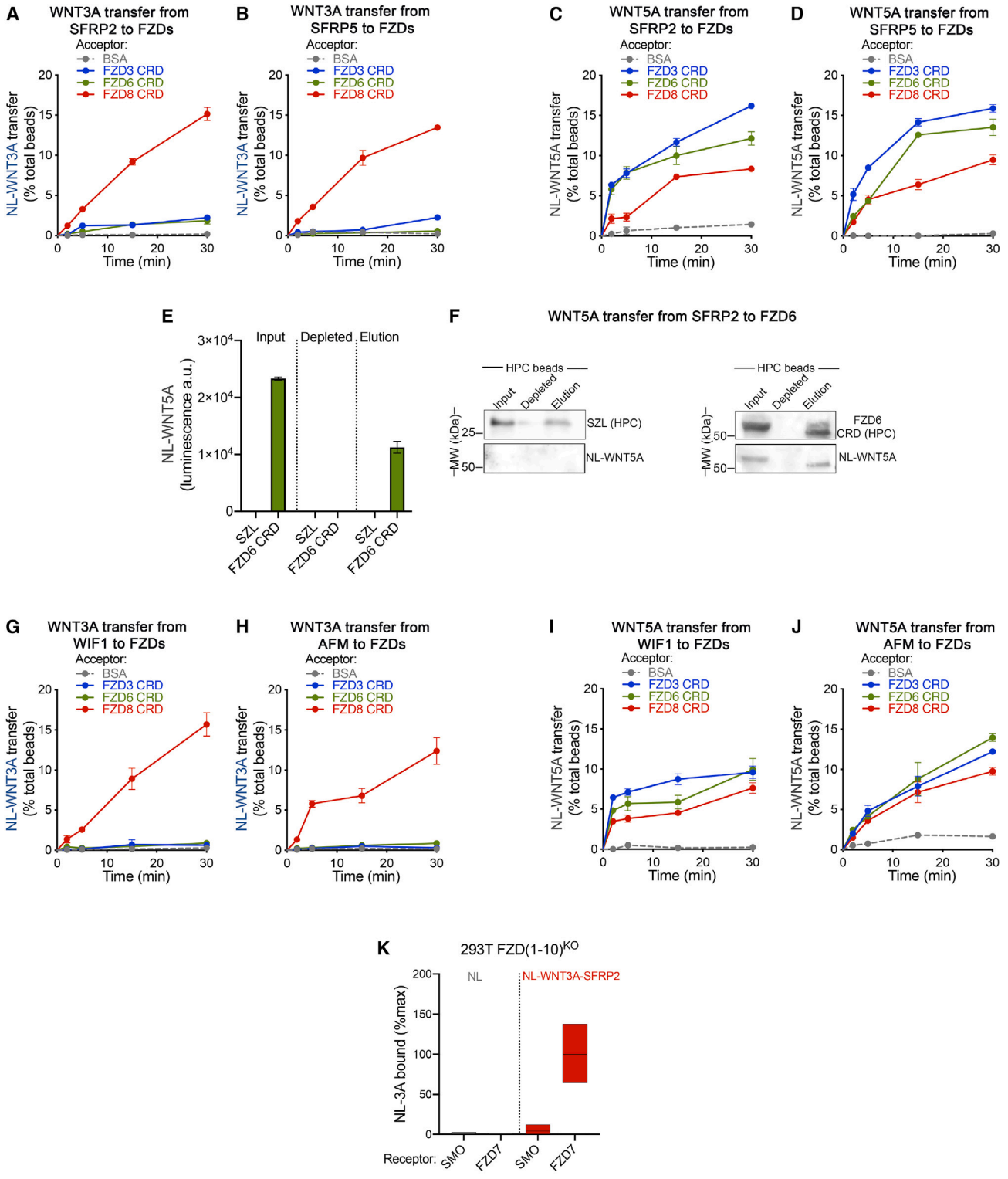

Figure 3. Carriers deliver canonical and non-canonical WNTs to FZDs

(A) NL-WNT3A-SFRP2 complexes were covalently captured on HaloLink beads, via HT7 attached to the C terminus of SFRP2. The beads were then incubated with purified FZD-CRDs (5 μM), and NL-WNT3A release was measured by NL luminescence. Incubation with BSA served as negative control. Canonical WNT3A shows a preference for transfer to FZD8-CRD. Points represent average for two biological and three technical replicates, normalized by total NL-WNT on beads, and error bars represent SD. See also Figures S4A–S4D for the activity of WNT3A-carrier complexes on FZD(1–10)^{KO} and WT cells rescued by the expression of FZD1-8 and for the purification of FZD-CRDs.

(legend continued on next page)

Please cite this article in press as: de Almeida Magalhaes et al., Extracellular carriers control lipid-dependent secretion, delivery, and activity of WNT morphogens, Developmental Cell (2023), https://doi.org/10.1016/j.devcel.2023.11.027

Malinauskas et al.,[31] and Lin et al.[32]). We have previously observed that the activity of Sonic Hedgehog (SHH)-SCUBE2 complexes is inhibited by large excesses of lipid-dependent SHH binders.[42] We thus wondered if a similar effect explains WNT antagonism by SFRPs and WIF1. Indeed, the activity of all WNT3A carrier complexes, including WNT3A-AFM, was inhibited in a dose-dependent manner by an "empty" carrier (Figures 2F and 2G). These data indicate that carriers are inhibitory at high molar excess, as expected if they compete with WNT-FZD binding (Figure 2H).

Specific carrier-mediated WNT delivery to FZDs

Canonical and non-canonical WNTs signal through distinct FZDs.[9,47] We next asked if carriers can deliver WNTs to FZDs, and whether delivery is specific. We first determined which FZDs support signaling by canonical WNT3A-SFRP2 and WNT3A-WIF1 complexes, by performing rescue experiments in FZD-null (FZD(1–10)^{KO}) cells.[48] As expected, FZD(1–10)^{KO} cells did not respond to WNT3A-SFRP2 or WNT3A-WIF1 (Figures S4A and S4B), which was reversed upon transfection of all FZDs except FZD3 and FZD6, consistent with previous work implicating FZD3 and FZD6 in non-canonical Wnt signaling.[49]

We next tested whether carriers can transfer WNTs directly to FZDs, by incubating WNT carrier complexes captured on beads with purified FZD-CRDs (Figures S4C and S4D), which recapitulate WNT binding.[9] As shown in Figures 3A and 3B, canonical WNT3A was readily transferred from SFRP2 and SFRP5 to FZD8-CRD, but much less efficiently to FZD3-CRD and FZD6-CRD. In contrast, non-canonical WNT5A was preferentially transferred to FZD3-CRD and FZD6-CRD (Figures 3C and 3D). By immunoprecipitating acceptor FZD-CRDs, we confirmed that they form stable complexes with the transferred WNT (Figures 3E, 3F, and S4E–S4G). Similar results were obtained when WIF1 and AFM were used as donors (Figures 3G–3J). Finally, we asked whether WNT transfer from carriers to FZDs occurs on cells. As shown in Figure 3K, a NL-WNT3A-SFRP2 efficiently and specifically delivered NL-WNT3A to FZD(1–10)^{KO} cells rescued with FZD7. Together, these results indicate that WNTs can be transferred from carriers to FZDs and that the transfer of canonical and non-canonical WNTs is driven by the specificity of WNT-FZD interaction.

A subset of GPCs is required for vertebrate Wnt signaling

Dlp plays an essential role in Wnt reception in *Drosophila*,[50] binding Wg in a lipid-dependent manner.[25] In contrast to vertebrates, however, flies do not have SFRPs, and their WIF1 homolog, Shifted (Shf), is not involved in Wnt signaling.[51] We thus asked whether vertebrate GPCs are involved in signaling by WNT carrier complexes, by knocking out all six GPCs in cultured human cells (Table S1). As shown in Figures 4A, 4B, S4H, and S4I, GPC(1–6)^{KO} cells displayed a strong defect in WNT responsiveness, which was robustly rescued by GPC1, GPC4, or GPC6 (Figures S4J and S4K). Thus, one or more of a subset of GPCs is required for Wnt signaling in mammalian cells.

GPCs facilitate WNT transfer from carriers to FZDs

Since GPCs are expected to function upstream of FZDs, we first asked whether GPCs can accept WNTs from carriers. Indeed, both WNT3A and WNT5A were rapidly transferred from carriers to purified GPC4 and GPC6 ectodomains (Figures 4C and S4L–S4O), forming stable complexes (Figures 4D and 4E). Consistent with this result, SFRP2 delivered NL-WNT3A specifically to GPC(1–6)^{KO} cells rescued with GPC4 or GPC6 (Figure 4F). We also observed reverse WNT transfer from GPC4-ecto to SFRP2, as expected from a mass action-driven process (Figures 4G and S4P); however, GPCs were better acceptors than SFRP2 (Figures 4C, 4G, and S4M–S4P). Thus, although WNT transfer from carriers to GPCs is reversible, forward transfer is favored, perhaps by higher affinity of GPCs for WNT.

We next asked if GPCs can transfer WNTs to FZDs. As shown in Figures 4H, 4I, S4Q, and S4R, GPC4- and GPC6-ecto readily donated WNT3A to FZD8, and WNT5A to FZD3 and FZD6. Importantly, purified WNT3A-GPC4-ecto (Figure S4S) activated Wnt signaling (Figure 4J). Finally, we asked whether GPCs might facilitate WNT movement from carriers to FZDs. Small amounts of GPC4-ecto strongly potentiated NL-WNT3A transfer from SFRP2 or WIF1 to FZD8 (Figures 4K and S5A). Similar results were obtained for NL-WNT5A transfer from carriers to FZD3 and FZD6 (Figures 4L, 4M, S5B, and S5C). In contrast, GPC2, GPC3, or GPC5 ectodomains (Figure S5D) did not affect NL-WNT transfer from SFRP2 to FZDs (Figures 4N–4P and S5E–S5J). These data demonstrate that a subset of GPCs catalyze WNT movement from carriers to FZDs.

(B) As in (A), but with NL-WNT3A-SFRP5 on beads.
(C) As in (A) but with NL-WNT5A-SFRP2 on beads. Non-canonical WNT5A is preferentially transferred to FZD3-CRD and FZD6-CRD.
(D) As in (C), but with NL-WNT5A-SFRP5 on beads.
(E) Beads carrying NL-WNT5A-SFRP2 were incubated with HPC-tagged FZD6-CRD or Sizzled (SZL, negative control), which were then immunopurified from the supernatant using anti-HPC antibodies, followed by elution with HPC peptide. Samples were analyzed by NL luminescence. Input and depleted samples represent the supernatant before and after incubation with anti-HPC beads, whereas the elution sample represents the peptide eluate. NL-WNT5A forms a stable complex with FZD6-CRD after release from SFRP2. Points represent average for two biological and technical replicates, and error bars represent SD. See Figures S4E and S4F for SZL purification and a similar experiment showing NL-WNT3A transfer from SFRP2 to FZD8-CRD.
(F) As in (E) but samples were analyzed by SDS-PAGE and immunoblotting. See Figure S4G for WNT3A and FZD8-CRD immunoblotting.
(G) As in (A), but with NL-WNT3A-WIF1 on beads.
(H) As in (A), but with NL-WNT3A-AFM on beads.
(I) As in (A), but with NL-WNT5A-WIF1 on beads.
(J) As in (A), but with NL-WNT5A-AFM on beads.
(K) FZD(1–10)^{KO} cells expressing eGFP-tagged FZD7 or Smoothened (SMO, negative control) were incubated with purified NL-WNT3A-SFRP2 for 1 h, and NL-WNT3A bound to cells was quantified by anti-NL immunofluorescence. NL-WNT3A is delivered to cells expressing FZD7, but not SMO. Data are normalized between background signal (incubation with NL) and maximum NL-WNT3A binding (100%). Points represent average binding for one biological and four technical replicates, and error bars represent SEM. At least 300 cells were quantified per replicate.
See Figures S4A–S4G for the additional characterization of signaling activity by WNT3A-carrier complexes.

Please cite this article in press as: de Almeida Magalhaes et al., Extracellular carriers control lipid-dependent secretion, delivery, and activity of WNT morphogens, Developmental Cell (2023), https://doi.org/10.1016/j.devcel.2023.11.027

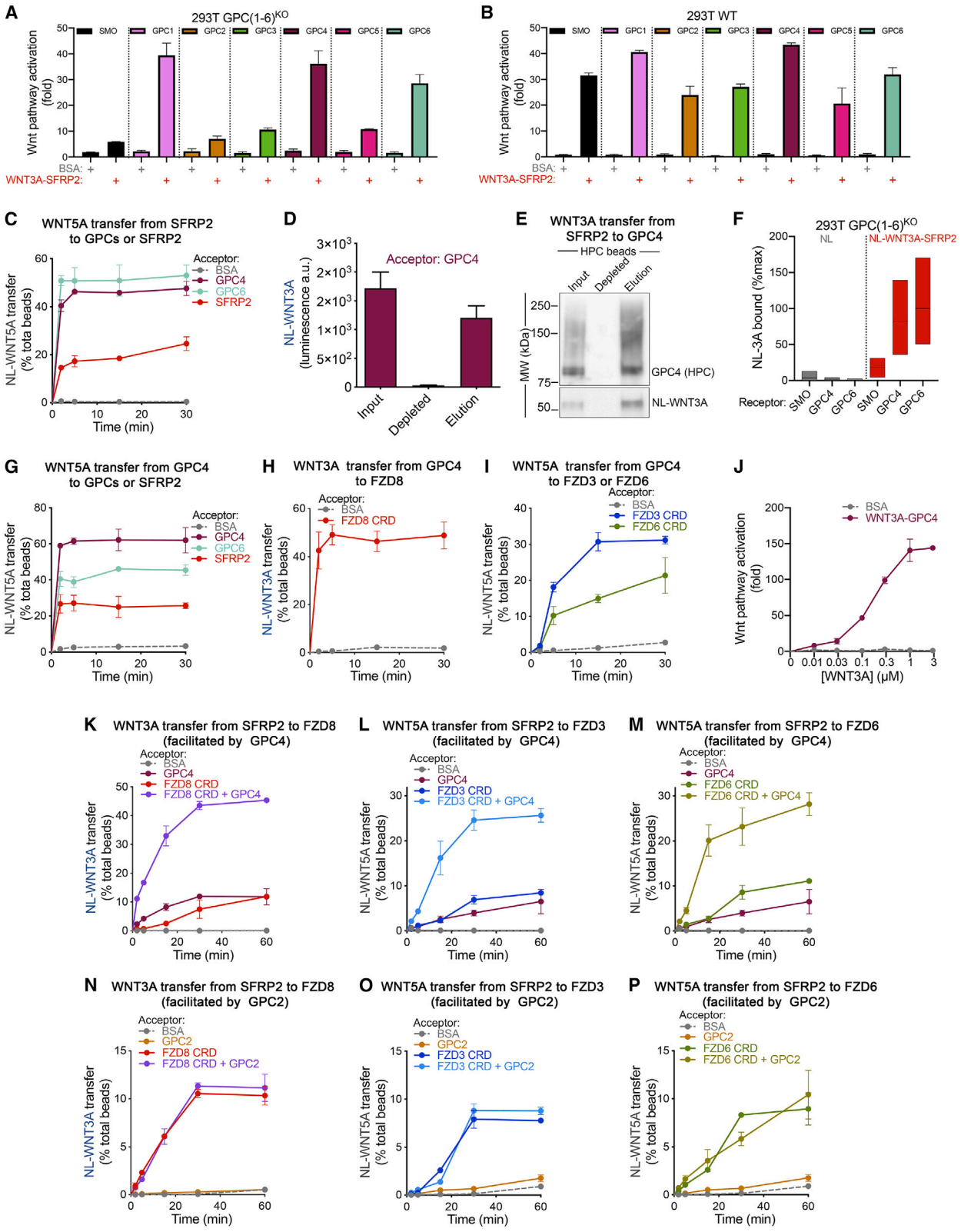

Figure 4. Glypicans are required for Wnt signaling and facilitate WNT transfer from carriers to FZDs

(A) Wnt pathway activation by purified WNT3A-SFRP2 (1 μM) was measured in GPC(1–6)^{KO} cells. Wnt responsiveness is impaired in the absence of GPCs and is rescued by the expression of eGFP-tagged GPC1, GPC4 or GPC6, but not SMO (negative control). Bars represent average activation for two biological and

(legend continued on next page)

Please cite this article in press as: de Almeida Magalhaes et al., Extracellular carriers control lipid-dependent secretion, delivery, and activity of WNT morphogens, Developmental Cell (2023), https://doi.org/10.1016/j.devcel.2023.11.027

Glycosaminoglycan chains are not necessary for GPC activity

Glycosaminoglycan (GAG) chains are prominent GPC modifications, but their role in Wnt signaling is unclear.[25,52,53] We used our previously described strategy[54] to purify GPC4-ecto produced by cells lacking (1) exostosin-1 (EXT1), a glycosyltransferase required for heparan sulfate (HS) chain elongation; (2) chondroitin sulfate N-acetylgalactosaminyltransferases 1 and 2 (CSGALNACT1 and CSGALNACT2), required for chondroitin sulfate (CS) chain elongation; or (3) beta-1,3-glucuronyltransferase 3 (B3GAT3), required for attachment of both HS and CS chains to the GPC protein core (Figure 5A). Unmodified GPC4-ecto behaved indistinguishably from GAG-modified species in accepting WNTs from SFRP2 (Figures 5B and S5K) and transferring them to FZDs (Figures 5C and S5L). Additionally, all GPC4 species catalyzed WNT transfer from SFRP2 to FZDs, irrespective of GAG modification (Figures 5D–5G and S5M–S5P). Finally, complexes of WNT3A with different GPC4-ecto species showed similar signaling activity (Figure 5H). These results indicate that GAG chains are dispensable for the function of GPCs in vertebrate Wnt signaling.

Carriers transfer WNTs to NOTUM, promoting WNT inactivation

NOTUM hydrolyzes the palmitoleate moiety of WNTs.[26] Past biochemical studies relied on detergents for providing WNT substrates to NOTUM.[26] A key unanswered question is how WNTs are delivered to NOTUM physiologically. We first tested if NOTUM might accept WNTs directly from WLS, similar to carriers. Wild-type NOTUM or a catalytically inactive point mutant (NOTUM^{S232A})[26] (Figures S6A and S6B) were unable to release WNT from cells (Figure S6C), indicating that NOTUM cannot receive WNTs from WLS. We next asked whether carriers can deliver WNTs to NOTUM. As shown in Figures 6A, 6B, S6D, and S6E, NL-WNT3A and NL-WNT5A were robustly transferred from SFRP2, AFM, and WIF1 to NOTUM. The catalytically inactive mutant NOTUM^{S232A} was equally efficient in accepting WNTs from carriers (Figures 6A, 6B, S6D, and S6E), indicating that transfer did not require hydrolysis of the lipid moiety. Interestingly, both wild-type NOTUM and NOTUM^{S232A} were immunoprecipitated with the WNT3A-SFRP2 complex (Figure 6C) but not with SFRP2 (Figure 6D), suggesting a transfer intermediate in which WNT bridges SFRP2 and NOTUM.

Finally, we asked whether NOTUM inactivates WNTs delivered by carriers. As shown in Figures 6E–6G and S6F, incubation with NOTUM inhibited the activity of WNT3A-carrier complexes in a dose-dependent manner. As expected, WNT3A-carrier complexes retained activity when incubated with NOTUM^{S232A} (Figures 6E–6G). However, NOTUM^{S232A} became inhibitory at high excess (Figures S6G and S6H), consistent with binding lipidated WNTs. Together, these results demonstrate that carriers deliver WNT substrates to NOTUM, resulting in WNT inactivation.

The WNT3A-SFRP5 complex is refractory to NOTUM inhibition

In contrast to all other WNT carriers, SFRP5 did not efficiently deliver WNTs to NOTUM (Figures 6H and 6I). Consistent with this result, NOTUM and NOTUM^{S232A} showed much reduced binding to WNT3A-SFRP5 compared with WNT3A-SFRP2

technical replicates, normalized to untreated cells, and error bars represent SD. See Figures S4H–S4K for the expression of eGFP-tagged constructs and additional Wnt activity assays in GPC(1–6)^{KO} cells.

(B) As in (A), but with WT cells.

(C) NL-WNT5A-SFRP2 was covalently captured on beads via SFRP2, followed by incubation with 5 μM GPC4-ecto, GPC6-ecto, SFRP2, or BSA (negative control). NL-WNT5A release into the supernatant was measured by luminescence. NL-WNT5A is transferred robustly from SFRP2 to GPCs, but less efficiently to other SFRP2 molecules. Points represent average of two biological and three technical replicates, normalized by total NL-WNT on beads, and error bars represent SD. See also Figures S4L–S4O for protein purification and additional characterization of NL-WNT transfer between carriers and GPCs.

(D) NL-WNT3A-SFRP2 beads were incubated with HPC-tagged GPC4-ecto, and the supernatant was subjected to anti-HPC immunoprecipitation, followed by elution with HPC peptide. NL luminescence was measured in the supernatant before (input) and after (depleted) immunoprecipitation, and in the peptide eluate. NL-WNT3A forms a stable complex with GPC4-ecto after release from SFRP2. Points represent average for two biological and technical replicates, and error bars represent SD.

(E) As in (D), but samples were analyzed by SDS-PAGE and immunoblotting.

(F) GPC(1–6)^{KO} expressing eGFP-tagged GPC4, GPC6, or SMO (negative control) were treated with purified NL-WNT3A-SFRP2 for 1 h, and bound ligand was quantified by anti-NL immunofluorescence. Incubation with purified NL served as background control. NL-WNT3A is transferred to GPC4 and GPC6 on cells. Data are normalized between NL background signal and maximum NL-WNT binding (100%). Points represent average of one biological and four technical replicates, and error bars represent SEM. At least 300 cells were measured per replicate.

(G) As in (C), but with NL-WNT5A-GPC4-ecto on beads. NL-WNT5A is efficiently transferred to other GPC molecules, but less efficiently to SFRP2.

(H) As in (C), but NL-WNT3A-GPC4-ecto beads were incubated with purified FZD8-CRD (5 μM). NL-WNT3A is robustly transferred from GPC4 to FZD8. See Figure S4Q for NL-WNT3A transfer from GPC6 to FZD8-CRD.

(I) As in (H), but NL-WNT5A-GPC4-ecto beads were incubated with purified FZD3-CRD or FZD6-CRD (5 μM). See Figure S4R for NL-WNT5A-GPC6 beads.

(J) Wnt pathway activation by purified WNT3A-GPC4-ecto (0.01, 0.03, 0.1, 0.3, 1, and 3 μM with respect to WNT3A), assayed on reporter cells. Points represent average activation for two biological and technical replicates, normalized to untreated cells, and error bars represent SD. See Figure S4S for purification of WNT3A-GPC4-ecto complex.

(K) As in (C), but NL-WNT3A-SFRP2 beads were incubated with FZD8-CRD (5 μM), with or without GPC4-ecto (0.5 μM). Small amounts of GPC4-ecto potentiate WNT3A transfer from SFRP2 to FZD8-CRD. See Figure S5A for a similar experiment using NL-WNT3A-WIF1.

(L) As in (K), but with NL-WNT5A-SFRP2 beads incubated with FZD3-CRD (5 μM). See also Figure S5B for a similar experiment using NL-WNT5A-WIF1.

(M) As in (L), but with NL-WNT5A-SFRP2 beads incubated with FZD6-CRD (5 μM). See Figure S5C for NL-WNT5A-WIF1 transfer on beads.

(N) As in (K), but NL-WNT3A-SFRP2 beads were incubated with or without GPC2-ecto (0.5 μM). Small amounts of GPC2-ecto do not potentiate WNT3A transfer from SFRP2 to FZD8-CRD. See Figures S5D–S5J for protein purification and similar experiments using GPC3-ecto or GPC5-ecto.

(O) As in (N), but NL-WNT5A-SFRP2 beads were incubated with FZD3-CRD (5 μM).

(P) As in (O), but NL-WNT5A-SFRP2 beads were incubated with FZD6-CRD (5 μM).

See Figures S4H–S4S and S5A–S5J for additional characterization of WNT transfer from SFRPs, WIF1, and GPCs to receptors and co-receptors.

Please cite this article in press as: de Almeida Magalhaes et al., Extracellular carriers control lipid-dependent secretion, delivery, and activity of WNT morphogens, Developmental Cell (2023), https://doi.org/10.1016/j.devcel.2023.11.027

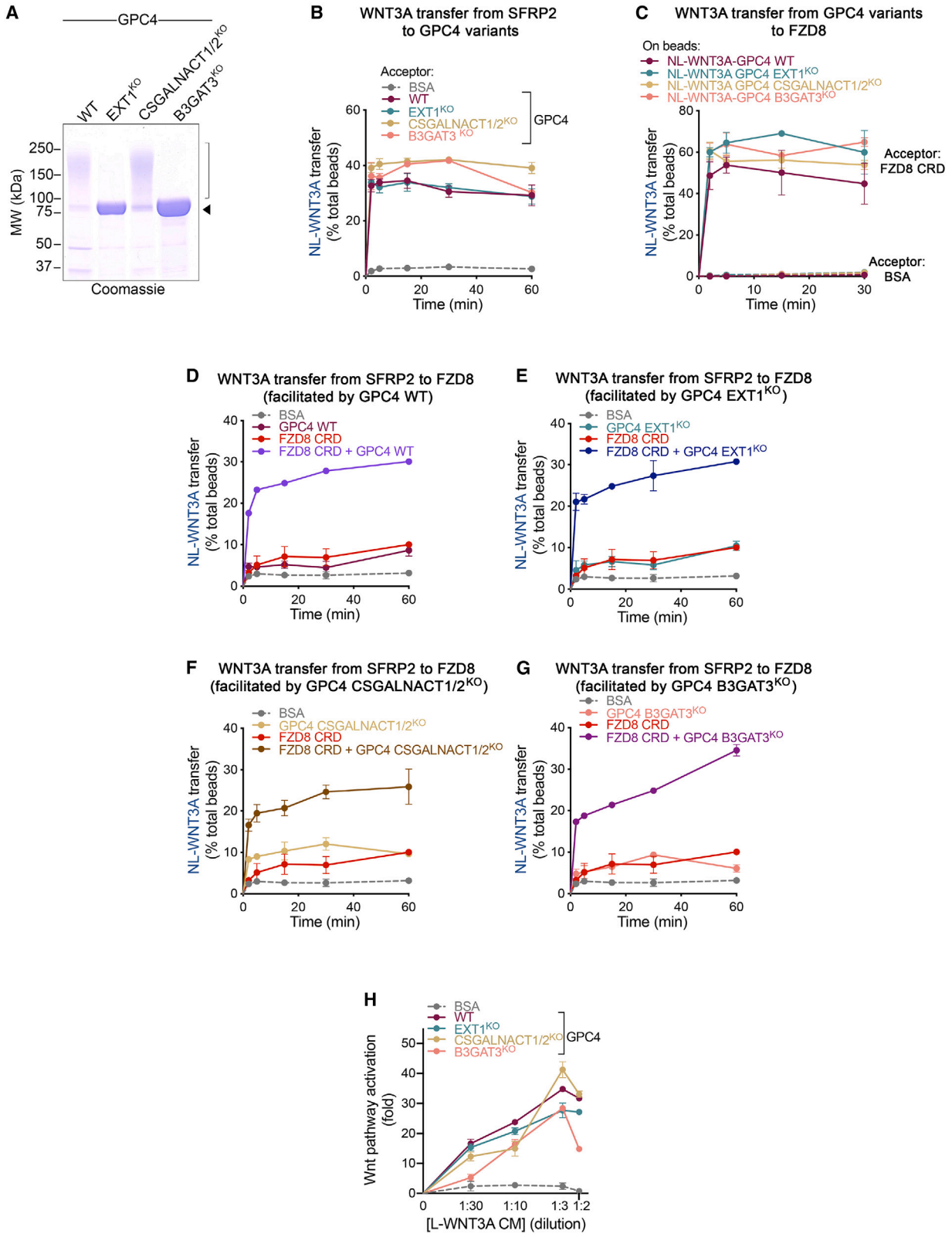

Figure 5. The core protein recapitulates the function of GPCs in Wnt signaling

(A) GPC4-ecto was expressed in WT, EXT1^{KO}, CSGALNACT1/2^{KO}, or B3GAT3^{KO} cells. The proteins were affinity-purified and then analyzed by SDS-PAGE and Coomassie staining. Arrowhead indicates the unmodified GPC4-ecto core protein and bracket indicates GAG-modified species.

(legend continued on next page)

Please cite this article in press as: de Almeida Magalhaes et al., Extracellular carriers control lipid-dependent secretion, delivery, and activity of WNT morphogens, Developmental Cell (2023), https://doi.org/10.1016/j.devcel.2023.11.027

(Figures 6J and 6K). Importantly, purified NOTUM had drastically reduced inhibitory activity against WNT3A-SFRP5 (Figure 6L). If WNT3A-SFRP5 is resistant to NOTUM because WNT3A transfer is impaired, rescuing transfer should restore WNT3A sensitivity to NOTUM. Since WNTs are readily transferred from SFRP5 to WIF1 (Figures S6I and S6J), we reasoned that WIF1 should bypass the block to WNT transfer from SFRP5 to NOTUM. Indeed, a low amount of WIF1 (0.2 μM) dramatically rescued transfer of both WNT3A and WNT5A from SFRP5 to NOTUM (Figures 6M and S6K). Moreover, WIF1 restored inhibition of WNT3A-SFRP5 by NOTUM (Figure 6N). These data demonstrate that uniquely among WNT carriers, SFRP5 does not donate to NOTUM, allowing WNTs to escape repression by it.

Stable WNT3A complexes promote growth and maintenance of intestinal organoids

Intestinal organoid culture requires canonical Wnt stimulation, usually by WNT3A-conditioned media[55] or purified WNT3A solubilized in CHAPS detergent.[19] Both these preparations are not ideal: conditioned media is undesirable for serum-sensitive assays, whereas detergent limits long-term stability and suppresses stem cell self-renewal.[34,35] We thus investigated whether purified WNT3A complexes support human intestinal organoid expansion. Gratifyingly, WNT3A-SFRP1 and WNT3A-GPC4-ecto maintained growth (Figure 7A) and high organoid number (Figure 7B) over 3 passages, similar to WNT3A-conditioned media. In contrast, commercial WNT3A and other WNT3A-carrier complexes did not support prolonged organoid expansion. Paralleling the effects on organoid expansion, activity of WNT3A-SFRP1 and WNT3A-GPC4-ecto on reporter cells was higher than that of the other WNT3A sources (Figures S7A–S7C). Dramatically, WNT3A-carrier complexes retained activity after a 48-h incubation at room temperature or even at 37°C, in contrast to commercial WNT3A, which lost activity precipitously (Figures 7C and S7D).

To optimize using WNT3A-carrier complexes for intestinal organoid culture, we tested the effect of reducing the number of media changes. WNT3A-SFRP1 and WNT3A-GPC4-ecto supported growth (Figure S7E), higher organoid number (Figure S7F), and higher cell viability (Figure S7G) over multiple passages, with only twice weekly media changes, outperforming WNT3A-conditioned media. To determine if WNT3A-SFRP1 and WNT3A-GPC4-ecto maintain stem cells and Wnt pathway activation in organoids, we analyzed LGR5[56] and β-catenin levels,[57] respectively. Compared with other WNT3A preparations, WNT3A-SFRP1 and WNT3A-GPC4-ecto showed stronger induction of LGR5 and β-catenin (Figures 7D and S7H). Finally, since organoid culture requires large amounts of WNT3A, we optimized the production of WNT3A-GPC4-ecto complexes in Expi293 suspension cells,[58] by co-expressing WNT3A, GPC4-ecto, and PORCN using modular cloning technology.[59] This approach afforded purified WNT3A-GPC4-ecto in high yield (0.14 mg/mL of medium) (Figure S7I). The complex thus produced was potent in signaling (Figure S7J) and supported robust intestinal organoid propagation and stem cell maintenance (Figures S7K and S7L). Thus, purified WNT3A-carrier complexes are stable and support long-term stem cell maintenance and intestinal organoid growth.

DISCUSSION

WNT morphogens are modified with palmitoleate, which is critical for signaling[19,60] but causes aqueous insolubility. How WNTs are released from cells, to signal non-cell autonomously, has long been an open question. Furthermore, WNT insolubility has been a major obstacle in obtaining active WNTs. Our results define the molecular mechanisms by which WNTs are solubilized, regulated extracellularly, and delivered to target cells. We propose the following pathway for the movement of WNTs during vertebrate embryonic signaling. In producing cells, PORCN attaches palmitoleate to WNTs,[21,61,62] which are then escorted by WLS to the plasma membrane.[23,24,63] Next, WNTs are handed off from WLS to secreted carriers belonging to SFRP and WIF1 families (Figure 7E), which use their lipid-binding domains to shield the palmitoleate moiety from the aqueous environment. Soluble WNT carrier complexes spread from producing cells through extracellular space, reaching the surface of distant cells, where they activate Wnt signaling (Figure 7F). Although WNTs can be directly unloaded from carriers to FZDs, the process is greatly facilitated by GPCs, which accept WNTs from carriers and, in turn, transfer them to FZDs. In support of this model, we find that the vertebrate GPC family is critical for Wnt pathway activation. Finally, carriers can also promote inactivation of WNTs, by transferring them to NOTUM[26] (Figure 7G). Thus, a dedicated network of extracellular lipid-binding proteins shuttle WNTs between spatially segregated effectors and regulators.

The high signaling potency of WNT carrier complexes stands in contrast to the role primarily attributed to SFRPs[30,32,64] and

(B) NL-WNT3A-SFRP2 complexes on beads were incubated with 5 μM GPC4-ecto purified from WT, EXT1^{KO}, CSGALNACT1/2^{KO}, or B3GAT3^{KO} cells, or BSA (negative control). NL-WNT3A release was measured at different time points by NL luminescence. NL-WNT3A is transferred from SFRP2 to all GPC4-ecto variants. Points represent average for two biological and three technical replicates, normalized by total NL-WNT on beads, and error bars represent SD. See also Figure S5K for NL-WNT5A transfer.

(C) As in (B), but beads carrying NL-WNT3A-GPC4-ecto variants were incubated with FZD8-CRD (5 μM). All GPC4-ecto variants donate NL-WNT3A to FZD8-CRD. See Figure S5L for a similar experiment using NL-WNT5A-GPC4-ecto variants.

(D) As in (B), but NL-WNT3A-SFRP2 beads were incubated with FZD8-CRD (5 μM), with or without GPC4-ecto from WT cells (0.3 μM). Small amounts of GPC4-ecto from WT cells potentiate WNT3A transfer from SFRP2 to FZD8-CRD. See Figure S5M for a similar experiment using NL-WNT5A-SFRP2.

(E) As in (D), but with purified GPC4-ecto from EXT1^{KO} cells (0.3 μM). See Figure S5N for NL-WNT5A-SFRP2 on beads.

(F) As in (D), but with purified GPC4-ecto from CSGALNACT1/2^{KO} cells (0.3 μM). See Figure S5O for NL-WNT5A-SFRP2 transfer on beads.

(G) As in (D), but with purified GPC4-ecto from B3GAT3^{KO} cells (0.3 μM). See Figure S5P for NL-WNT5A transfer.

(H) GPC4-ecto variants (1 μM) or BSA (negative control) were added to L-WNT3A cells, and Wnt signaling activity was measured in serial dilutions of the conditioned media. All GPC4-ecto variants release active WNT3A. Points represent average activation for two biological and three technical replicates, normalized to untreated reporter cells, and error bars represent SD.

See Figures S5K–S5P for additional characterization of the role of GPC GAG modification in Wnt signaling.

Please cite this article in press as: de Almeida Magalhaes et al., Extracellular carriers control lipid-dependent secretion, delivery, and activity of WNT morphogens, Developmental Cell (2023), https://doi.org/10.1016/j.devcel.2023.11.027

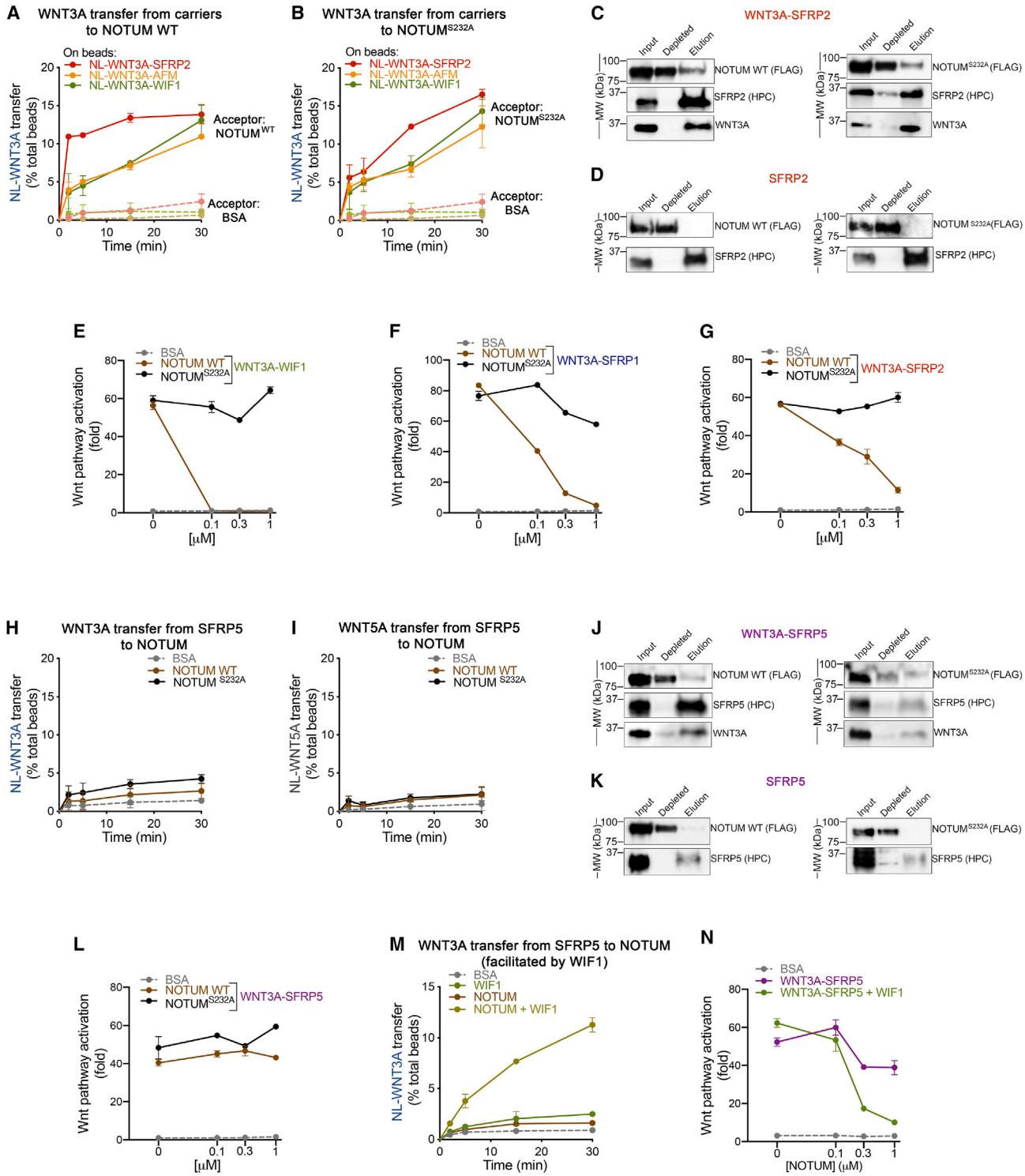

Figure 6. Carriers deliver WNT substrates to NOTUM

(A) NL-WNT3A complexes with SFRP2, AFM, or WIF1 on beads were incubated with 5 μM wild-type (WT) NOTUM or BSA (negative control), and NL-WNT release was measured by NL luminescence. NL-WNT3A is transferred from carriers to NOTUM. Points represent average for two biological and three technical replicates, normalized by total NL-WNT on beads, and error bars represent SD. See Figures S6A–S6E for additional purification and characterization of NOTUM.

(B) As in (A), but showing NL-WNT3A transfer to enzymatically inactive NOTUM^{S232A}.

(C) Purified WNT3A-SFRP2 (6 μM) was incubated with FLAG-tagged NOTUM WT or NOTUM^{S232A} (3 μM), followed by immunoprecipitation with antibodies against the HPC tag on SFRP2. Samples were analyzed by SDS-PAGE and immunoblotting. NOTUM proteins interact with WNT3A-SFRP2.

(legend continued on next page)

Please cite this article in press as: de Almeida Magalhaes et al., Extracellular carriers control lipid-dependent secretion, delivery, and activity of WNT morphogens, Developmental Cell (2023), https://doi.org/10.1016/j.devcel.2023.11.027

WIF1[29,31] as WNT antagonists. We find that all WNT carriers indeed inhibit signaling at large molar excess over the ligand, as earlier reported for SFRP1.[65] Interestingly, overexpressed SFRP promotes WNT spreading in early *Xenopus* embryos,[66] consistent with our finding that SFRPs promote WNT secretion. Finally, some loss-of-function phenotypes indicate a positive role of SFRPs in Wnt signaling *in vivo*.[67,68] These results suggest that SFRPs and WIF1 can function to either promote or inhibit WNT activity, depending on concentration. Future studies will be needed to elucidate how various carriers control Wnt pathway output in different contexts.

WNT carriers promote the secretion of both canonical and non-canonical WNTs. Additionally, WNT transfer from carriers to FZDs is dictated not by carrier but by the preferred formation of canonical or non-canonical ligand-receptor pairs. In responding cells, interactions between WNTs and components of the receptor complex (LRP5/6 for canonical and ROR1/2 for non-canonical WNTs) further contribute to WNT specificity. Thus, like PORCN and WLS, WNT carriers are perhaps general for all WNTs, irrespective of functional classification. A notable exception is SFRP5, which forms WNT complexes resistant to inhibition by NOTUM, due to impaired WNT handoff (Figure 7G). It is currently unknown how this feature of SFRP5 is implicated in NOTUM-dependent WNT regulation *in vivo*. What might account for the unique behavior of SFRP5? Investigations of the mechanism of cholesterol handoff between the soluble lysosomal protein NPC2 and the N-terminal luminal domain of the cholesterol transporter NPC1 identified surface residues in NPC2 required for cholesterol handoff to NPC1.[69] Perhaps similarly, specific residues in SFRPs are involved in WNT transfer to NOTUM, and these residues are not conserved in SFRP5. Future experiments will be needed to define the molecular basis of WNT handoff from carriers to NOTUM and other acceptors.

WNT secretion shows intriguing similarities to that of Hedgehog (Hh) ligands.[42] Both Wnt and Hh ligands are lipid-modified and are released in complex with a carrier, one of the proteins described here, or a SCUBE family protein, respectively. In both cases, ligand-carrier complex formation is catalyzed by a dedicated membrane protein, WLS and Dispatched-1 (DISP1), respectively. Perhaps, the carriers are sterically hindered from "picking up" the lipid-modified ligands directly from the membrane, thus requiring presentation by WLS or DISP1. This is a simple but effective mechanism for ensuring that Wnt and Hh morphogens do not diffuse from producing cells in an uncontrolled fashion.

At the level of target cells, we find that a subset of vertebrate GPCs is essential for the response to WNTs; interestingly, the GPC core protein suffices for this role, whereas the GAG chains are dispensable. This represents another parallel between Wnt and Hh signaling. The mechanism employed by GPCs in WNT reception is reminiscent of that of GAS1 in the Hh pathway.[70] Both GPCs and GAS1 function as pre-receptors, shuttling a lipidated ligand from an extracellular carrier to a primary receptor but are not themselves components of the final signaling complex. Such a catalytic mechanism for ligand-receptor complex assembly ensures that low amounts of GPCs or GAS1 can have large effects on cellular responsiveness to ligands. It remains to be elucidated how GPC levels modulate Wnt pathway output *in vivo*.

When not membrane-embedded, the WNT palmitoleate moiety appears always shielded from the aqueous environment by interaction with a binding partner, likely to avoid aggregation. Interestingly, the lipid-dependent interactions of WNTs investigated here are highly dynamic, allowing WNT handoff between binders, including between identical molecules, on the order of minutes or less; this situation is also reminiscent of Hh ligands.[42] Aside from allowing rapid deployment of an otherwise insoluble molecule, we speculate that the dynamic exchange between carriers suggests a possible mechanism for directional WNT propagation along a gradient of carriers immobilized to the extracellular matrix, as proposed for Hh morphogens.[42]

WNT lipidation is conserved between vertebrates and *Drosophila*, as are requirements for WLS in WNT secretion and for GPCs in WNT reception. In contrast to vertebrates, however, *Drosophila* does not have SFRP and AFM homologs, whereas the *Drosophila* WIF1 homolog, Shf, is specifically involved in long-range Hh signaling.[51,71] How are then *Drosophila* WNTs delivered to target cells? It is possible that yet to be discovered extracellular proteins function as WNT carriers in *Drosophila*. Alternatively, Wnt ligands might be transferred only between neighboring cells, by handoff between Dlp molecules anchored to closely apposed plasma membranes.[25]

Two major routes have been proposed for the long-range movement of WNTs in tissues. One route involves WNT mobilization from producing cells by carriers, such as exosomes,[36,37] lipoproteins,[38] or dedicated proteins (this study), followed by

(D) As in (B) but with SFRP2 (6 μM). NOTUM proteins do not interact with SFRP2.
(E) WNT3A-WIF1 (1 μM) was incubated with varying concentrations of purified NOTUM WT or NOTUM^{S232A} or with BSA (1 μM, negative control), after which signaling activity was measured on reporter cells. WT NOTUM inhibits activity of WNT3A-carrier in dose-dependent manner. Points represent average activation for two biological and three technical replicates, normalized to untreated cells, and error bars represent SD. See also Figures S6F–S6H for additional characterization of the effect of NOTUM on WNT3A-carriers.
(F) As in (E), but with purified WNT3A-SFRP1 complex.
(G) As in (E), but with purified WNT3A-SFRP2 complex.
(H) As in (A), but with beads carrying NL-WNT3A-SFRP5. SFRP5 cannot efficiently transfer NL-WNT3A to NOTUM proteins.
(I) As in (H), but with NL-WNT5A-SFRP5 on beads.
(J) As in (C), but with WNT3A-SFRP5. Binding of NOTUM proteins to WNT3A-SFRP5 is much reduced compared with WNT3A-SFRP2.
(K) As in (D), but with SFRP5.
(L) As in (E), but with purified WNT3A-SFRP5 (1 μM). WNT3A-SFRP5 activity is much less sensitive to inhibition by NOTUM.
(M) As in (H), but with addition of WIF1 (0.2 μM). Small amounts of WIF1 rescue transfer of WNT3A from SFRP5 to NOTUM. See Figures S6I–S6K for the additional characterization of NL-WNT-SFRP5 beads.
(N) As in (L) but with addition of WIF1 (0.1 μM). Small amount of WIF1 restore the ability of NOTUM to inhibit WNT3A-SFRP5 activity.
See Figure S6 for additional the characterization of WNT delivery to NOTUM by carriers.

Please cite this article in press as: de Almeida Magalhaes et al., Extracellular carriers control lipid-dependent secretion, delivery, and activity of WNT morphogens, Developmental Cell (2023), https://doi.org/10.1016/j.devcel.2023.11.027

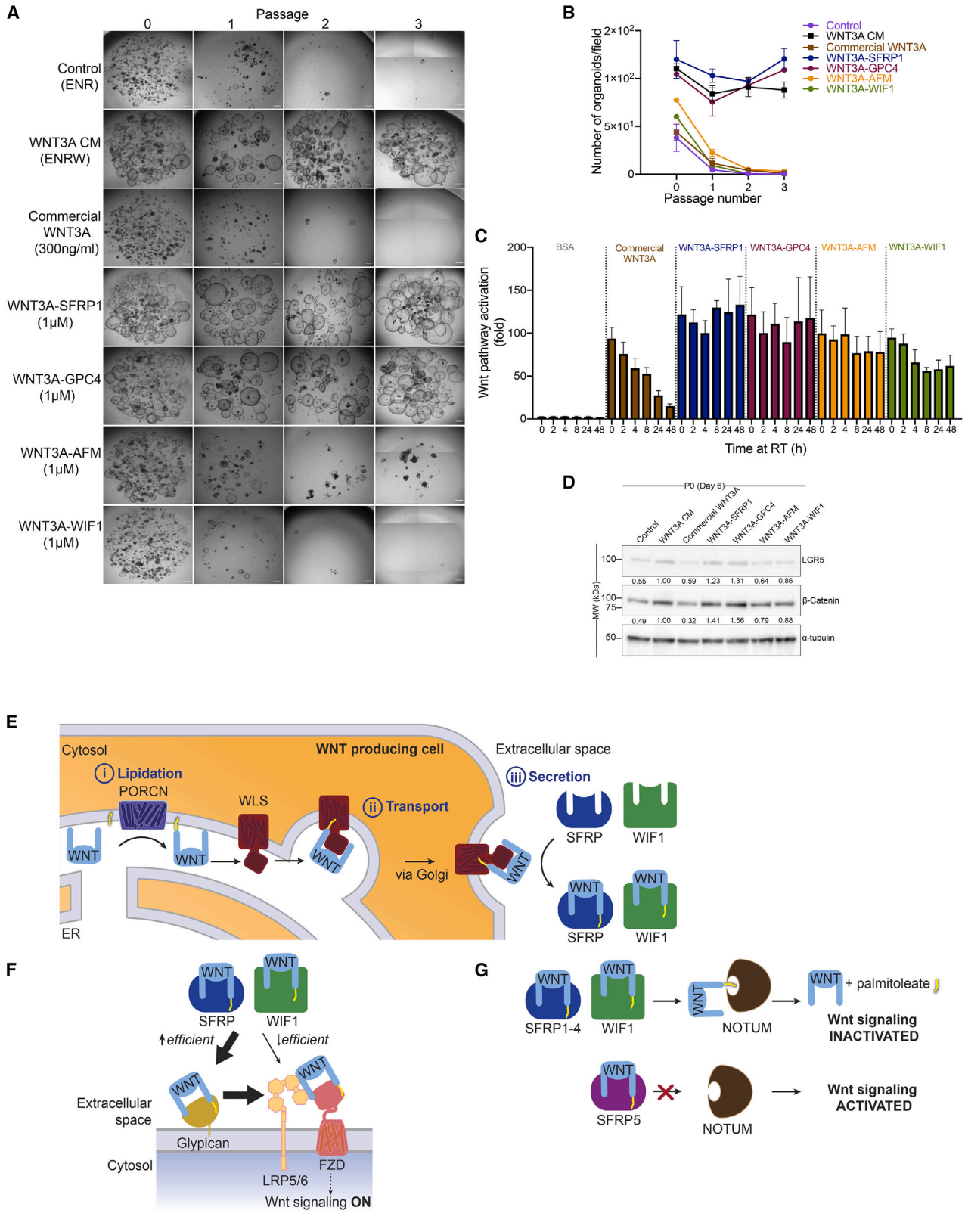

Figure 7. WNT3A-carrier complexes support human intestinal organoid growth and maintenance

(A) Representative images of human intestinal organoids grown for three passages in ENR (EGF, Noggin, and R-spondin) media supplemented with various WNT3A preparations. WNT3A-carrier complexes were added at 1 μM and commercial WNT3A at 300 ng/mL.[40] Scale bars, 500 μm.

(legend continued on next page)

diffusion to target cells, through extracellular space. Another route is represented by cytonemes,[39] on which WNTs spread without leaving the surface of the producing cell. However, WNTs transported along cytonemes would then need to be transferred to target cells. We envision that the two routes outlined above can complement each other: cytonemes provide physical support for transporting WNTs at a distance, after which extracellular carrier proteins catalyze WNT movement from the cytoneme membrane to the target cell.

Finally, our results have practical implications for obtaining defined, active, and stable WNT preparations, devoid of serum or detergents. Some of the complexes described here support prolonged growth of human intestinal organoids, outperforming commercial WNT3A and WNT3A-conditioned media. It is unclear why WNT3A-AFM is ineffective in maintaining organoid growth in our hands, in contrast to a previous report[41]; we speculate that differences in tissue biopsy, age of donors, or cultivation protocol might account for the discrepancy. It is currently unknown whether carriers can potentiate endogenous Wnt signaling in differentiated intestinal organoids, especially whether carriers are involved in WNT3A movement from Paneth cells to neighboring WNT-responsive Lgr5+ intestinal stem cells. We envision that the remarkable stability of WNT carrier complexes will enable *in vitro* studies and potential applications in regenerative medicine.

Limitations of the study

(1) We show that two families of extracellular proteins release WNTs in soluble and active form and deliver them to GPC co-receptors. The specificity of this system is unknown: we do not understand whether individual carriers and GPCs prefer different WNTs. (2) The study does not address the nature of endogenous WNT morphogens during embryogenesis, especially the question of the molar ratio between WNT and carriers, which dictates signaling output. (3) Although we have a structural understanding of WNT recognition by WLS, carriers, NOTUM, and GPCs, the precise mechanisms of WNT transfer between these proteins are unknown. (4) It is unknown if and how WNT handoffs are regulated *in vivo* to control Wnt pathway output; future work will investigate how the molecular mechanisms described here are deployed in different developmental settings.

STAR★METHODS

Detailed methods are provided in the online version of this paper and include the following:

SUPPLEMENTAL INFORMATION

Supplemental information can be found online at https://doi.org/10.1016/j.devcel.2023.11.027.

ACKNOWLEDGMENTS

We thank A. Elseht for assistance with organoids culture, Harvard Medical School Cell Biology Initiative for Genome Editing and Neurodegeneration for support with gene editing, and B. Vanhollebeke for the gift of FZD(1–10)^{KO} cells. P.H. is a CPRIT Scholar in Cancer Research supported by the Cancer Prevention and Research Institute of Texas (CPRIT) grant RR200080. This work was supported by NIH grant R01GM122920-05, R35GM153357-01 to A.S and Cell Biology Education and Goldberg Fellowship Fund to T.d.A.M.

AUTHOR CONTRIBUTIONS

T.d.A.M., J.L., B.M.W., and A.S. designed reagents and experiments. T.d.A.M. and J.L. generated reagents, purified proteins, and performed WNT release and activity assays and image analysis. T.d.A.M. performed WNT transfer and immunoprecipitation experiments. J.L. generated WLS^{KO} HEK293. C.C. performed modular cloning and Expi293 cell transfection and created the WNT cartoons. A.J.K. performed modular cloning. K.S.B., P.M., and D.Z. performed human intestinal organoid experiments. J.Z. generated GPC(1–6)^{KO} HEK293 cells. Y.G., Z.L., and P.H. purified WLS-WNT5A complex. R.W. provided reagents and data. D.T.B. provided reagents, data,

(B) Organoid numbers for experiment in (A). Points represent average number of organoids in two wells, and error bars represent SD.
(C) WNT3A preparations (1 μM) and commercial WNT3A (300 ng/mL) were incubated at room temperature for the indicated time, after which signaling activity was measured on reporter cells. Activity of WNT3A-carrier complexes does not appreciably decrease after 48 h, in contrast to commercial WNT3A. Points represent average Wnt pathway activation for two biological and technical replicates, normalized to untreated cells, and error bars represent SD.
(D) LGR5 and β-catenin expression in the experiment in (A) was analyzed by immunoblotting at passage 0 (day 6). Blotting for α-tubulin served as loading control.
(E) Model for WNT secretion. Following lipidation by PORCN in the ER (i), WNTs are escorted to the cell surface by WLS (ii). WNTs are then directly transferred to carriers (SFRPs, WIF1, and AFM) (iii).
(F) Model for WNT delivery to FZDs. Carriers donate WNTs to GPCs, which then hand WNTs off to FZDs. WNTs can also be transferred directly from carriers to FZDs, but less efficiently than via GPC-catalyzed transfer. Specificity of WNT-FZD interaction contributes to whether a given WNT activates canonical or non-canonical signaling.
(G) Model for WNT inhibition by NOTUM. Carriers discharge WNTs to NOTUM, which inactivates them. SFRP5 cannot transfer WNTs to NOTUM, rendering them refractory to this inhibitory mechanism.
See Figure S7 for additional data on long-term stability of WNT3A-carrier complexes and use for organoid culture.

consultation, and access to the organoid core. T.d.A.M. and A.S. analyzed data. T.d.A.M. and A.S. wrote the manuscript.

DECLARATION OF INTERESTS

The authors declare no competing interests.

Received: March 15, 2023
Revised: August 29, 2023
Accepted: November 30, 2023
Published: December 27, 2023

REFERENCES

1. Stapornwongkul, K.S., and Vincent, J.P. (2021). Generation of extracellular morphogen gradients: the case for diffusion. Nat. Rev. Genet. *22*, 393–411.
2. Wiese, K.E., Nusse, R., and van Amerongen, R. (2018). Wnt signalling: conquering complexity. Development *145*, dev165902.
3. Beachy, P.A., Karhadkar, S.S., and Berman, D.M. (2004). Tissue repair and stem cell renewal in carcinogenesis. Nature *432*, 324–331.
4. Clevers, H., Loh, K.M., and Nusse, R. (2014). Stem cell signaling. An integral program for tissue renewal and regeneration: Wnt signaling and stem cell control. Science *346*, 1248012.
5. Baron, R., and Kneissel, M. (2013). WNT signaling in bone homeostasis and disease: from human mutations to treatments. Nat. Med. *19*, 179–192.
6. Mullor, J.L., Sánchez, P., and Ruiz i Altaba, A. (2002). Pathways and consequences: Hedgehog signaling in human disease. Trends Cell Biol. *12*, 562–569.
7. Bale, A.E. (2002). Hedgehog signaling and human disease. Annu. Rev. Genomics Hum. Genet. *3*, 47–65.
8. Mirabelli, C.K., Nusse, R., Tuveson, D.A., and Williams, B.O. (2019). Perspectives on the role of Wnt biology in cancer. Sci. Signal. *12*, eaay4494.
9. Janda, C.Y., Waghray, D., Levin, A.M., Thomas, C., and Garcia, K.C. (2012). Structural basis of Wnt recognition by Frizzled. Science *337*, 59–64.
10. Niehrs, C. (2012). The complex world of WNT receptor signalling. Nat. Rev. Mol. Cell Biol. *13*, 767–779.
11. Chen, S., Bubeck, D., MacDonald, B.T., Liang, W.X., Mao, J.H., Malinauskas, T., Llorca, O., Aricescu, A.R., Siebold, C., He, X., and Jones, E.Y. (2011). Structural and functional studies of LRP6 ectodomain reveal a platform for Wnt signaling. Dev. Cell *21*, 848–861.
12. Cheng, Z., Biechele, T., Wei, Z., Morrone, S., Moon, R.T., Wang, L., and Xu, W. (2011). Crystal structures of the extracellular domain of LRP6 and its complex with DKK1. Nat. Struct. Mol. Biol. *18*, 1204–1210.
13. Cong, F., Schweizer, L., and Varmus, H. (2004). Wnt signals across the plasma membrane to activate the beta-catenin pathway by forming oligomers containing its receptors, Frizzled and LRP. Development *131*, 5103–5115.
14. Janda, C.Y., Dang, L.T., You, C., Chang, J., de Lau, W., Zhong, Z.A., Yan, K.S., Marecic, O., Siepe, D., Li, X., et al. (2017). Surrogate Wnt agonists that phenocopy canonical Wnt and beta-catenin signalling. Nature *545*, 234–237.
15. Sheetz, J.B., Mathea, S., Karvonen, H., Malhotra, K., Chatterjee, D., Niininen, W., Perttilä, R., Preuss, F., Suresh, K., Stayrook, S.E., et al. (2020). Structural insights into pseudokinase domains of receptor tyrosine kinases. Mol. Cell *79*, 390–405.e7.
16. Shi, F., Mendrola, J.M., Sheetz, J.B., Wu, N., Sommer, A., Speer, K.F., Noordermeer, J.N., Kan, Z.Y., Perry, K., Englander, S.W., et al. (2021). ROR and RYK extracellular region structures suggest that receptor tyrosine kinases have distinct WNT-recognition modes. Cell Rep. *37*, 109834.
17. Veeman, M.T., Axelrod, J.D., and Moon, R.T. (2003). A second canon. Dev. Cell *5*, 367–377.
18. Ho, H.Y., Susman, M.W., Bikoff, J.B., Ryu, Y.K., Jonas, A.M., Hu, L., Kuruvilla, R., and Greenberg, M.E. (2012). Wnt5a-Ror-Dishevelled signaling constitutes a core developmental pathway that controls tissue morphogenesis. Proc. Natl. Acad. Sci. USA *109*, 4044–4051.
19. Willert, K., Brown, J.D., Danenberg, E., Duncan, A.W., Weissman, I.L., Reya, T., Yates, J.R., 3rd, and Nusse, R. (2003). Wnt proteins are lipid-modified and can act as stem cell growth factors. Nature *423*, 448–452.
20. Zhai, L., Chaturvedi, D., and Cumberledge, S. (2004). Drosophila wnt-1 undergoes a hydrophobic modification and is targeted to lipid rafts, a process that requires porcupine. J. Biol. Chem. *279*, 33220–33227.
21. Kadowaki, T., Wilder, E., Klingensmith, J., Zachary, K., and Perrimon, N. (1996). The segment polarity gene porcupine encodes a putative multitransmembrane protein involved in Wingless processing. Genes Dev. *10*, 3116–3128.
22. Tanaka, K., Okabayashi, K., Asashima, M., Perrimon, N., and Kadowaki, T. (2000). The evolutionarily conserved porcupine gene family is involved in the processing of the Wnt family. Eur. J. Biochem. *267*, 4300–4311.
23. Bänziger, C., Soldini, D., Schütt, C., Zipperlen, P., Hausmann, G., and Basler, K. (2006). Wntless, a conserved membrane protein dedicated to the secretion of Wnt proteins from signaling cells. Cell *125*, 509–522.
24. Nygaard, R., Yu, J., Kim, J., Ross, D.R., Parisi, G., Clarke, O.B., Virshup, D.M., and Mancia, F. (2021). Structural basis of WLS/Evi-mediated Wnt transport and secretion. Cell *184*, 194–206.e14.
25. McGough, I.J., Vecchia, L., Bishop, B., Malinauskas, T., Beckett, K., Joshi, D., O'Reilly, N., Siebold, C., Jones, E.Y., and Vincent, J.P. (2020). Glypicans shield the Wnt lipid moiety to enable signalling at a distance. Nature *585*, 85–90.
26. Kakugawa, S., Langton, P.F., Zebisch, M., Howell, S., Chang, T.H., Liu, Y., Feizi, T., Bineva, G., O'Reilly, N., Snijders, A.P., et al. (2015). Notum deacylates Wnt proteins to suppress signalling activity. Nature *519*, 187–192.
27. Leyns, L., Bouwmeester, T., Kim, S.H., Piccolo, S., and De Robertis, E.M. (1997). Frzb-1 is a secreted antagonist of Wnt signaling expressed in the Spemann organizer. Cell *88*, 747–756.
28. Wang, S., Krinks, M., and Moos, M., Jr. (1997). Frzb-1, an antagonist of Wnt-1 and Wnt-8, does not block signaling by Wnts -3A, -5A, or -11. Biochem. Biophys. Res. Commun. *236*, 502–504.
29. Hsieh, J.C., Rattner, A., Smallwood, P.M., and Nathans, J. (1999). Biochemical characterization of Wnt-frizzled interactions using a soluble, biologically active vertebrate Wnt protein. Proc. Natl. Acad. Sci. USA *96*, 3546–3551.
30. Dann, C.E., Hsieh, J.C., Rattner, A., Sharma, D., Nathans, J., and Leahy, D.J. (2001). Insights into Wnt binding and signalling from the structures of two Frizzled cysteine-rich domains. Nature *412*, 86–90.
31. Malinauskas, T., Aricescu, A.R., Lu, W., Siebold, C., and Jones, E.Y. (2011). Modular mechanism of Wnt signaling inhibition by Wnt inhibitory factor 1. Nat. Struct. Mol. Biol. *18*, 886–893.
32. Lin, K., Wang, S., Julius, M.A., Kitajewski, J., Moos, M., Jr., and Luyten, F.P. (1997). The cysteine-rich frizzled domain of Frzb-1 is required and sufficient for modulation of Wnt signaling. Proc. Natl. Acad. Sci. USA *94*, 11196–11200.
33. Peters, C., Wolf, A., Wagner, M., Kuhlmann, J., and Waldmann, H. (2004). The cholesterol membrane anchor of the Hedgehog protein confers stable membrane association to lipid-modified proteins. Proc. Natl. Acad. Sci. USA *101*, 8531–8536.
34. Dhamdhere, G.R., Fang, M.Y., Jiang, J., Lee, K., Cheng, D., Olveda, R.C., Liu, B., Mulligan, K.A., Carlson, J.C., Ransom, R.C., et al. (2014). Drugging a stem cell compartment using Wnt3a protein as a therapeutic. PLoS One *9*, e83650.
35. Tüysüz, N., van Bloois, L., van den Brink, S., Begthel, H., Verstegen, M.M., Cruz, L.J., Hui, L., van der Laan, L.J., de Jonge, J., Vries, R., et al. (2017). Lipid-mediated Wnt protein stabilization enables serum-free culture of human organ stem cells. Nat. Commun. *8*, 14578.
36. Greco, V., Hannus, M., and Eaton, S. (2001). Argosomes: a potential vehicle for the spread of morphogens through epithelia. Cell *106*, 633–645.

37. Gross, J.C., Chaudhary, V., Bartscherer, K., and Boutros, M. (2012). Active Wnt proteins are secreted on exosomes. Nat. Cell Biol. *14*, 1036–1045.

38. Panáková, D., Sprong, H., Marois, E., Thiele, C., and Eaton, S. (2005). Lipoprotein particles are required for Hedgehog and Wingless signalling. Nature *435*, 58–65.

39. Stanganello, E., Hagemann, A.I., Mattes, B., Sinner, C., Meyen, D., Weber, S., Schug, A., Raz, E., and Scholpp, S. (2015). Filopodia-based Wnt transport during vertebrate tissue patterning. Nat. Commun. *6*, 5846.

40. Komekado, H., Yamamoto, H., Chiba, T., and Kikuchi, A. (2007). Glycosylation and palmitoylation of Wnt-3a are coupled to produce an active form of Wnt-3a. Genes Cells *12*, 521–534.

41. Mihara, E., Hirai, H., Yamamoto, H., Tamura-Kawakami, K., Matano, M., Kikuchi, A., Sato, T., and Takagi, J. (2016). Active and water-soluble form of lipidated Wnt protein is maintained by a serum glycoprotein afamin/alpha-albumin. Elife *5*, e11621.

42. Wierbowski, B.M., Petrov, K., Aravena, L., Gu, G., Xu, Y., and Salic, A. (2020). Hedgehog pathway activation requires coreceptor-catalyzed, lipid-dependent relay of the sonic Hedgehog ligand. Dev. Cell *55*, 450–467.e8.

43. Wawrzak, D., Métioui, M., Willems, E., Hendrickx, M., de Genst, E., and Leyns, L. (2007). Wnt3a binds to several sFRPs in the nanomolar range. Biochem. Biophys. Res. Commun. *357*, 1119–1123.

44. Petrov, K., Wierbowski, B.M., Liu, J., and Salic, A. (2020). Distinct cation gradients power cholesterol transport at different key points in the Hedgehog signaling pathway. Dev. Cell *55*, 314–327.e7.

45. Taipale, J., Chen, J.K., Cooper, M.K., Wang, B., Mann, R.K., Milenkovic, L., Scott, M.P., and Beachy, P.A. (2000). Effects of oncogenic mutations in Smoothened and Patched can be reversed by cyclopamine. Nature *406*, 1005–1009.

46. Xu, Q., Wang, Y., Dabdoub, A., Smallwood, P.M., Williams, J., Woods, C., Kelley, M.W., Jiang, L., Tasman, W., Zhang, K., and Nathans, J. (2004). Vascular development in the retina and inner ear: control by Norrin and Frizzled-4, a high-affinity ligand-receptor pair. Cell *116*, 883–895.

47. Wu, C.H., and Nusse, R. (2002). Ligand receptor interactions in the Wnt signaling pathway in Drosophila. J. Biol. Chem. *277*, 41762–41769.

48. Eubelen, M., Bostaille, N., Cabochette, P., Gauquier, A., Tebabi, P., Dumitru, A.C., Koehler, M., Gut, P., Alsteens, D., Stainier, D.Y.R., et al. (2018). A molecular mechanism for Wnt ligand-specific signaling. Science *361*, eaat1178.

49. Dong, B., Vold, S., Olvera-Jaramillo, C., and Chang, H. (2018). Functional redundancy of frizzled 3 and frizzled 6 in planar cell polarity control of mouse hair follicles. Development *145*, dev168468.

50. Franch-Marro, X., Marchand, O., Piddini, E., Ricardo, S., Alexandre, C., and Vincent, J.P. (2005). Glypicans shunt the Wingless signal between local signalling and further transport. Development *132*, 659–666.

51. Glise, B., Miller, C.A., Crozatier, M., Halbisen, M.A., Wise, S., Olson, D.J., Vincent, A., and Blair, S.S. (2005). Shifted, the Drosophila ortholog of Wnt inhibitory factor-1, controls the distribution and movement of Hedgehog. Dev. Cell *8*, 255–266.

52. Reichsman, F., Smith, L., and Cumberledge, S. (1996). Glycosaminoglycans can modulate extracellular localization of the wingless protein and promote signal transduction. J. Cell Biol. *135*, 819–827.

53. Yan, D., Wu, Y., Feng, Y., Lin, S.C., and Lin, X. (2009). The core protein of glypican Dally-like determines its biphasic activity in wingless morphogen signaling. Dev. Cell *17*, 470–481.

54. Liu, Y.C., Wierbowski, B.M., and Salic, A. (2022). Hedgehog pathway modulation by glypican 3-conjugated heparan sulfate. J. Cell Sci. *135*, jcs.259297.

55. Sato, T., Stange, D.E., Ferrante, M., Vries, R.G., Van Es, J.H., Van den Brink, S., Van Houdt, W.J., Pronk, A., Van Gorp, J., Siersema, P.D., and Clevers, H. (2011). Long-term expansion of epithelial organoids from human colon, adenoma, adenocarcinoma, and Barrett's epithelium. Gastroenterology *141*, 1762–1772.

56. Barker, N., van Es, J.H., Kuipers, J., Kujala, P., van den Born, M., Cozijnsen, M., Haegebarth, A., Korving, J., Begthel, H., Peters, P.J., and Clevers, H. (2007). Identification of stem cells in small intestine and colon by marker gene Lgr5. Nature *449*, 1003–1007.

57. Sato, T., and Clevers, H. (2013). Growing self-organizing mini-guts from a single intestinal stem cell: mechanism and applications. Science *340*, 1190–1194.

58. Fang, X.T., Sehlin, D., Lannfelt, L., Syvänen, S., and Hultqvist, G. (2017). Efficient and inexpensive transient expression of multispecific multivalent antibodies in Expi293 cells. Biol. Proced. Online *19*, 11.

59. Jones, R.D., Qian, Y., Siciliano, V., DiAndreth, B., Huh, J., Weiss, R., and Del Vecchio, D. (2020). An endoribonuclease-based feedforward controller for decoupling resource-limited genetic modules in mammalian cells. Nat. Commun. *11*, 5690.

60. Takada, R., Satomi, Y., Kurata, T., Ueno, N., Norioka, S., Kondoh, H., Takao, T., and Takada, S. (2006). Monounsaturated fatty acid modification of Wnt protein: its role in Wnt secretion. Dev. Cell *11*, 791–801.

61. Rocheleau, C.E., Downs, W.D., Lin, R., Wittmann, C., Bei, Y., Cha, Y.H., Ali, M., Priess, J.R., and Mello, C.C. (1997). Wnt signaling and an APC-related gene specify endoderm in early C. elegans embryos. Cell *90*, 707–716.

62. Hofmann, K. (2000). A superfamily of membrane-bound O-acyltransferases with implications for Wnt signaling. Trends Biochem. Sci. *25*, 111–112.

63. Bartscherer, K., Pelte, N., Ingelfinger, D., and Boutros, M. (2006). Secretion of Wnt ligands requires Evi, a conserved transmembrane protein. Cell *125*, 523–533.

64. Bovolenta, P., Esteve, P., Ruiz, J.M., Cisneros, E., and Lopez-Rios, J. (2008). Beyond Wnt inhibition: new functions of secreted Frizzled-related proteins in development and disease. J. Cell Sci. *121*, 737–746.

65. Xavier, C.P., Melikova, M., Chuman, Y., Üren, A., Baljinnyam, B., and Rubin, J.S. (2014). Secreted Frizzled-related protein potentiation versus inhibition of Wnt3a/beta-catenin signaling. Cell. Signal. *26*, 94–101.

66. Mii, Y., and Taira, M. (2009). Secreted Frizzled-related proteins enhance the diffusion of Wnt ligands and expand their signalling range. Development *136*, 4083–4088.

67. Esteve, P., Sandonìs, A., Ibañez, C., Shimono, A., Guerrero, I., and Bovolenta, P. (2011). Secreted frizzled-related proteins are required for Wnt/beta-catenin signalling activation in the vertebrate optic cup. Development *138*, 4179–4184.

68. Sugiyama, Y., Shelley, E.J., Wen, L., Stump, R.J., Shimono, A., Lovicu, F.J., and McAvoy, J.W. (2013). Sfrp1 and Sfrp2 are not involved in Wnt/beta-catenin signal silencing during lens induction but are required for maintenance of Wnt/beta-catenin signaling in lens epithelial cells. Dev. Biol. *384*, 181–193.

69. Wang, M.L., Motamed, M., Infante, R.E., Abi-Mosleh, L., Kwon, H.J., Brown, M.S., and Goldstein, J.L. (2010). Identification of surface residues on Niemann-Pick C2 essential for hydrophobic handoff of cholesterol to NPC1 in lysosomes. Cell Metab. *12*, 166–173.

70. Huang, P., Wierbowski, B.M., Lian, T., Chan, C., García-Linares, S., Jiang, J., and Salic, A. (2022). Structural basis for catalyzed assembly of the Sonic hedgehog-Patched1 signaling complex. Dev. Cell *57*, 670–685.e8.

71. Gorfinkiel, N., Sierra, J., Callejo, A., Ibañez, C., and Guerrero, I. (2005). The Drosophila ortholog of the human Wnt inhibitor factor Shifted controls the diffusion of lipid-modified Hedgehog. Dev. Cell *8*, 241–253.

72. Ran, F.A., Hsu, P.D., Wright, J., Agarwala, V., Scott, D.A., and Zhang, F. (2013). Genome engineering using the CRISPR-Cas9 system. Nat. Protoc. *8*, 2281–2308.

73. Labun, K., Montague, T.G., Gagnon, J.A., Thyme, S.B., and Valen, E. (2016). CHOPCHOP v2: a web tool for the next generation of CRISPR genome engineering. Nucleic Acids Res. *44*, W272–W276.

74. Montague, T.G., Cruz, J.M., Gagnon, J.A., Church, G.M., and Valen, E. (2014). CHOPCHOP: a CRISPR/Cas9 and TALEN web tool for genome editing. Nucleic Acids Res. *42*, W401–W407.

75. Farin, H.F., Jordens, I., Mosa, M.H., Basak, O., Korving, J., Tauriello, D.V., de Punder, K., Angers, S., Peters, P.J., Maurice, M.M., and Clevers, H. (2016). Visualization of a short-range Wnt gradient in the intestinal stem-cell niche. Nature *530*, 340–343.

76. Los, G.V., Encell, L.P., McDougall, M.G., Hartzell, D.D., Karassina, N., Zimprich, C., Wood, M.G., Learish, R., Ohana, R.F., Urh, M., et al. (2008). HaloTag: a novel protein labeling technology for cell imaging and protein analysis. ACS Chem. Biol. *3*, 373–382.

77. Ohana, R.F., Encell, L.P., Zhao, K., Simpson, D., Slater, M.R., Urh, M., and Wood, K.V. (2009). HaloTag7: a genetically engineered tag that enhances bacterial expression of soluble proteins and improves protein purification. Protein Expr. Purif. *68*, 110–120.

78. Zeve, D., Stas, E., de Sousa Casal, J., Mannam, P., Qi, W., Yin, X., Dubois, S., Shah, M.S., Syverson, E.P., Hafner, S., et al. (2022). Robust differentiation of human enteroendocrine cells from intestinal stem cells. Nat. Commun. *13*, 261.

Please cite this article in press as: de Almeida Magalhaes et al., Extracellular carriers control lipid-dependent secretion, delivery, and activity of WNT morphogens, Developmental Cell (2023), https://doi.org/10.1016/j.devcel.2023.11.027

STAR★METHODS

KEY RESOURCES TABLE

REAGENT or RESOURCE	SOURCE	IDENTIFIER
Antibodies		
Mouse monoclonal anti-FLAG-M1	ATCC	Cat# HB-9259; RRID: CVCL_J730
Mouse monoclonal anti-HPC	A.C. Kruse	N/A
Affinity-purified rabbit polyclonal anti-NanoLuc	This study	N/A
Rabbit monoclonal anti-WNT3A (clone C64F2)	Cell Signaling Technology	Cat# 2721S; RRID: AB_2215411
Rabbit monoclonal anti-β-catenin (clone D10A8)	Cell Signaling Technology	Cat# 8480; RRID: AB_11127855
Rat monoclonal anti-WNT5A (clone 442625)	R&D Systems	Cat# MAB645; RRID: AB_10571221
Rabbit monoclonal anti-LGR5 (clone EPR3065Y)	Abcam	Cat# ab75850; RRID: AB_1523716
Mouse monoclonal anti-β-actin (clone ACTBD11B7)	Santa Cruz Biotechnology	Cat# sc-81178; RRID: AB_2223230
Mouse monoclonal anti-α-tubulin (clone TU-02)	Santa Cruz Biotechnology	Cat# sc-8035; RRID: AB_ 628408
Bacterial and Virus Strains		
E. coli BL21 (DE3) pLysS	Sigma	Cat# 69451
Chemicals, Peptides, and Recombinant Proteins		
Bovine Serum Albumin (BSA)	New England Biolabs	Cat# B9000S
IWP-2 (PORCN inhibitor) (≥98%)	Sigma	Cat# I0536
Polyethylenimine (PEI), linear, MW=25000	Polysciences	Cat# 23966
Cycloheximide (≥94%)	Sigma	Cat# 01810
FLAG elution peptide: NH_2-DYKDDDDK-OH	Genscript	N/A
HPC elution peptide: NH_2-EDQVDPRLIDGK-OH	Genscript	N/A
HaloLink™ amine	Promega	Cat# P6741
Recombinant mouse WNT3A protein	R&D Systems	Cat# 1324-WN-010/CF
cOmplete™ mini, EDTA-free protease inhibitor tablets	Roche	Cat# 11836170001
See Table S3 for a list of proteins utilized in this study.	This paper	N/A
Critical Commercial Assays		
BCA Assay	G Biosciences	Cat# 786-570
Superose® 6 column	GE Healthcase	N/A
Superose™ 6 Increase 10/300 GL	Cytiva	Cat#29091596
HaloLink™ resin	Promega	Cat# G1914
Amicon Ultra-0.5 centrifugal filter unit – 10kDa cutoff	Millipore	Cat# UFC5010
Amicon Ultra-4 centrifugal filter unit – 10kDa cutoff	Millipore	Cat# UFC8010
Nano-Glo luciferase assay	Promega	Cat# N1120
Dual-Glo luciferase assay	Promega	Cat# E2940
CellTiter-Glo 3D Cell Viability Assay	Promega	Cat# G9683
Experimental Models: Cell Lines		
Human: HEK293T cells	ATCC	Cat# CRL-3216
Mouse: L-WNT3A cells	ATCC	Cat# CRL-2647
Mouse: MEF cells	ATCC	Cat# CRL-2907
Human: WLS^{KO} HEK293T cells	This study	N/A
Human:$FZD(1\text{-}10)^{KO}$ HEK293T cells	Benoit Vanhollebeke[48]	N/A
Human:$GPC(1\text{-}6)^{KO}$ HEK293T cells	This study	N/A
Insect: Sf9 cells	Expression Systems	Cat#94-001F
Human: HEK293S GnTI$^-$ cells	Thermo Fisher Scientific	Cat#A39249
Human: Expi293 cells	Thermo Fisher Scientific	Cat#A14527

(*Continued on next page*)

Continued

REAGENT or RESOURCE	SOURCE	IDENTIFIER
Oligonucleotides		
See Table S1 for a list CRISPR gRNA oligonucleotides and sequencing primers utilized in this study.	This study	N/A
Recombinant DNA		
See Table S2 for a list of all plasmids utilized in this study.	This study	N/A
Software and Algorithms		
FIJI	National Institutes of Health	http://fiji.sc; RRID: SCR_002285
Photoshop CS5	Adobe	https://www.adobe.com/products/photoshop.html; RRID: SCR_014199
Illustrator	Adobe	https://www.adobe.com/products/illustrator.html; RRID: SCR_010279
Prism 8	GraphPad	http://www.graphpad.com/; RRID: SCR_002798
EVOS FL Auto 2 Imaging System	Invitrogen	N/A
SoftMax Pro 5.4.1	Molecular Devices	N/A
MATLAB	MathWorks	http://www.mathworks.com/products/matlab/; RRID: SCR_001622
MetaMorph Microscopy Automation and Image Analysis Software	Molecular Devices	http://www.moleculardevices.com/Products/Software/Meta-Imaging-Series/MetaMorph.html; RRID: SCR_002368
Other		
Wallac VICTOR3™ microplate reader	Perkin-Elmer	N/A
10x PlanApo 0.45NA objective	Nikon	N/A
ECLIPSE Ti2-E microscope	Nikon	N/A
EVOS FL 2 Auto microscope	Invitrogen	N/A
2x Olympus 6.22 AMEP4751 objective lens	Invitrogen	N/A
SpectraMax® M3 Multi-Mode microplate reader	Molecular Devices	N/A
Neon Transfection System	Thermo Fisher Scientific	N/A
Neon™ Transfection System 10 μL Kit	Thermo Fisher Scientific	MPK1096
MiSeq System	Illumina	N/A
MiSeq Reagent Nano Kit v2 (300-cycles)	Illumina	MS-103-1001

RESOURCE AVAILABILITY

Lead Contact

Further information and requests for reagents should be directed to, and will be fulfilled by, the lead contact, Adrian Salic (asalic@hms.harvard.edu).

Materials availability

Plasmids and cell lines generated in this study are available upon request from the lead contact.

Data and code availability

This study did not generate datasets.

EXPERIMENTAL MODEL AND STUDY PARTICIPANT DETAILS

Cell culture

Human Embryonic Kidney (HEK293) cells, WNT3A-producing L cells (L-WNT3A) cells and mouse embryonic fibroblasts (MEFs) cells were from ATCC; HEK293S GnTI$^-$ and Expi293 cells were from Thermo Fisher Scientific. FZDs(1-10)^{KO} HEK293 cells[48] were a gift from Benoit Vanhollebeke (Université Libre, Bruxelles). EXT1^{KO}, CSGALNACT1/2^{KO} and B3GAT3 ^{KO} cells were previously described.[54] All cell lines except Expi293 were maintained under standard growth conditions (37°C, 5% CO_2) and were grown in DMEM (Corning) supplemented with 10% (v/v) fetal bovine serum (VWR) and penicillin/streptomycin (Corning). Expi293 cells were

Please cite this article in press as: de Almeida Magalhaes et al., Extracellular carriers control lipid-dependent secretion, delivery, and activity of WNT morphogens, Developmental Cell (2023), https://doi.org/10.1016/j.devcel.2023.11.027

grown in suspension in Expi293 media (Thermo Fisher Scientific) at 37°C, 8% CO_2 and 125 rpm, in plastic flasks with ventilated caps (Corning). HEK293 cells are female. L-WNT3A cells are male. The sex of the MEFs used in this study has not been determined.

Generation of stable cell lines

Stable cell lines were generated by lentiviral transduction. Genes of interest were subcloned into third-generation lentiviral vectors,[72] modified to encode resistance to different markers (blasticidin, puromycin or hygromycin). Lentiviruses were produced by transient transfection in HEK293 cells. Cells of interest were transduced by incubation with lentivirus for 48h, in the presence of polybrene (1μg/mL, Sigma). Stable cell populations were subsequently isolated by antibiotic selection for 72h. Expression of the desired construct was confirmed by immunofluorescence and/or immunoblotting.

Generation of CRISPR/Cas9 knockout (KO) lines

To knock out WLS, synthetic oligonucleotides (IDT) encoding gRNA sequences (Table S1) were annealed and cloned into pX459 (Addgene).[72] HEK293 cells were transiently transfected with the gRNA-expressing plasmids, after which puromycin selection was applied for 24h, to enrich for transfected cells. To knock out the GPC family, gBlocks (IDT) were cloned into pX458 (Addgene) and pU6-(BbsI)CBh-Cas9-T2A-mCherry (Addgene), to generate plasmids expressing gRNAs that target GPC1/5/4 and GPC2/3/6, respectively. HEK293 cells were first electroporated with the GPC1/5/4 gRNA-expressing plasmid, and GFP-positive cells were sorted and expanded. The resulting cell population was then electroporated with the GPC2/3/6 gRNA-expressing plasmid, and single mCherry-positive cells were sorted and expanded in 96-well plates. Clones containing the desired knockouts were identified by Illumina MiSeq and were further confirmed in functional assays. Genomic loci targeted by the gRNAs were PCR amplified using flanking primers (Table S1) designed with CHOPCHOP,[73,74] followed by MiSeq sequencing. Indels in the knockout cell lines are shown in Table S1.

METHOD DETAILS

Antibodies

The following antibodies were obtained commercially: rabbit anti-WNT3A and anti-β-catenin monoclonals (Cell Signaling Technology); rat anti-WNT5A monoclonal (R&D Systems); rabbit anti-LGR5 monoclonal (Abcam); mouse anti-β-actin and anti-α-tubulin monoclonals (Santa Cruz Biotechnology). Mouse anti-FLAG-M1 and anti-HPC monoclonals were a generous gift from Andrew C Kruse (Harvard Medical School). Polyclonal antibodies against NanoLuc (NL) luciferase were raised in rabbits (Cocalico) and were affinity-purified against NL attached to Affigel-15 beads (BioRad). For immunoblotting, primary antibodies were used at 1-2μg/mL in TBST [10mM Tris-HCl, pH 7.6; 150mM NaCl; 0.2% Triton X-100 (v/v)] with 5% non-fat dry milk (m/v). For blotting with mouse anti-FLAG-M1 and anti-HPC monoclonals, all buffers were supplemented with 2mM $CaCl_2$. HRP–conjugated secondary antibodies were used at 0.2μg/mL. Secondary antibodies used in this study were: sheep anti-mouse IgG–HRP (Jackson ImmunoResearch), goat anti-rat IgG–HRP (Advansta) and donkey anti-rabbit IgG–HRP (GE Healthcare). For immunofluorescence, Alexa Fluor 594-conjugated anti-rabbit secondary antibodies were used at 1μg/mL in TBST with 5% (m/v) BSA.

DNA constructs

Plasmids used in this study are shown in Table S2. Additional information is provided below.

Expression constructs were subcloned into a lentiviral expression vector, under the control of a human CMV promoter. Overlapping PCR was used to introduce mutations and to assemble gene fusions. DNA constructs were confirmed by Sanger sequencing. Constructs encoding (NL)-tagged WNTs consist of the influenza hemagglutinin signal sequence, a FLAG epitope immediately after the signal peptide cleavage site, NL sequence, and the WNT sequence following the signal peptide.[75] Hierarchical Golden Gate Assembly was used to generate a plasmid for co-expressing PORCN, WNT3A and HPC-tagged GPC4-ecto, as previously described.[59]

Protein expression and purification

The proteins utilized in this study, including tagging and purification are shown in Table S3. General purification procedures are described below.

Expression and purification of secreted proteins from HEK293 cells

Secreted proteins were stably or transiently expressed in HEK293 cells, and were affinity-purified from conditioned media. Proteins were tagged with one copy of the FLAG or the HPC epitope. Some fusions also included HaloTag7 (HT7),[76,77] for fluorescent labeling or capture on beads. Cells expressing secreted proteins were grown to confluency and were switched to media containing 1% FBS (v/v), or 1% FBS (v/v) and 1μg/ml heparin in the case of SFRP1 and SFRP5. Conditioned media were harvested every 2 days, for a total of 3-4 collections. Pooled conditioned media were supplemented with 2mM $CaCl_2$ and were centrifuged and passed through 0.22μm filters, to remove debris. Clarified media were loaded onto columns packed with anti-FLAG or anti-HPC affinity resin. After extensive washing with TBS with 2mM $CaCl_2$, bound protein was eluted with elution buffer (20mM HEPES, pH 7.5; 200mM NaCl; 5mM EDTA; 100μg/mL FLAG or HPC peptide). Eluted protein was concentrated using centrifugal filter units (Millipore), and some were further purified by gel filtration on Superose 6 (GE Healthcare). Fractions containing the desired species were pooled, concentrated to at least 1mg/mL, flash frozen in liquid nitrogen, and stored -80°C. For WNT3A-carrier and WNT3A-GPC complexes, concentration of WNT3A was determined by immunoblotting serial dilutions alongside a serial dilution of commercial carrier-free WNT3A protein (R&D Systems).

Please cite this article in press as: de Almeida Magalhaes et al., Extracellular carriers control lipid-dependent secretion, delivery, and activity of WNT morphogens, Developmental Cell (2023), https://doi.org/10.1016/j.devcel.2023.11.027

Expression and purification of WNT3A-GPC4-ecto complex from Expi293 cells

Expi293 cells were transiently transfected with a plasmid co-expressing PORCN, WNT3A and HPC-tagged GPC4-ecto, using *TransIT*®-293 Transfection Reagent (Mirus). After 48h, the cells were expanded in suspension culture for 7 days. The conditioned media was then collected and subjected to anti-HPC affinity purification, as described above.

Purification of WLS-WNT5A complex

Synthetic DNA fragments encoding codon-optimized full-length hWNT5A (C-terminally tagged with one FLAG epitope) and hWLS (C-terminally tagged with one HPC epitope) were cloned into pVLAD6, and BacMam viruses were produced in Sf9 cells according to the manufacturer's instructions (Expression Systems). For protein expression, the two BacMam viruses were used to co-infect 1-liter cultures of HEK293S GnTI$^-$ cells in Freestyle 293 medium (Thermo Fisher Scientific), at a density of 3x10^6 cells/mL. After 12 hours, 10mM sodium butyrate (Sigma-Aldrich) was added, to enhance protein expression, and the cells were further incubated at 30°C for 48 h before harvesting. Cell pellets were resuspended in solubilization buffer [20 mM HEPES, pH 7.5; 150 mM NaCl; and 2% glyco-diosgenin (GDN, Anatrace)] supplemented with EDTA-free protease inhibitor cocktail (Roche). After clarification by centrifugation at 100,000g, the supernatant was applied to an anti-HPC affinity column. The column was washed with solubilization buffer, and bound protein was eluted with HPC elution buffer [20 mM HEPES, pH 7.5; 150 mM NaCl; 0.02% GDN; 0.1mg/mL HPC peptide; 5 mM EDTA]. The eluate was then affinity-purified on an anti-FLAG M2 column (Sigma-Aldrich). The hWLS-hWNT5A complex eluted with FLAG elution buffer [20 mM HEPES, pH 7.5; 150 mM NaCl; 0.02% GDN; 0.1mg/mL FLAG peptide] was subjected to size-exclusion chromatography on a Superose 6 Increase 10/300 GL column (Cytiva), in gel filtration buffer [20 mM HEPES, pH 7.5; 150 mM NaCl; 0.02% GDN].

Immunoblotting

Protein samples were separated by denaturing electrophoresis on 4-20% Mini-PROTEAN TGX precast gels (Bio-Rad). Gels were soaked in transfer buffer [48mM Tris, pH 9.2; 39mM glycine; 1.3mM SDS; 20% (v/v) methanol], followed by semi-dry transfer (Trans-Blot SD, Bio-Rad) to nitrocellulose membranes (Millipore). Membranes were blocked in TBST with 5% non-fat dry milk, incubated with primary antibodies overnight at 4°C, and washed with TBST. Membranes were then incubated with secondary antibodies for 1h at room temperature and then washed with TBST and TBS prior to chemiluminescent detection.

WNT release assays

For immunoblotting-based release assays, HEK293 cells stably expressing WNT3A or WNT5A were washed thrice with serum-free DMEM, and were incubated for 24 h in serum-free DMEM supplemented with the indicated factors. WNT3A and WNT5A were immunoblotted in conditioned media and corresponding cell lysates. For NL-based release assays, HEK293 cells (WT, WLS^{KO} or WLS-rescued WLS^{KO}) stably expressing NL-tagged WNTs were incubated overnight in DMEM without serum. For short time release assays (under 45min), the cells were pre-treated with cycloheximide (100μg/mL, Sigma) for 30 min prior to addition of purified proteins. In general, WNT release from cells was saturable at 1μM added purified carrier. In experiments testing the role of PORCN, cells were pre-treated overnight with the PORCN inhibitor, IWP-2 (2μM, Sigma). Aliquots of conditioned media were collected in duplicate at the indicated times, centrifuged to remove cellular debris, and NL luciferase activity was measured using Nano-Glo Luciferase Assay Substrate (Promega), according to the manufacturer's instructions. NL-tagged WNT released into the media was normalized using the total NL signal in the corresponding cells, harvested at the end of the time course.

Canonical Wnt pathway reporter assay

Activity of various WNT3A complexes was assayed using a stable MEF line harboring a β-catenin-activated reporter (pBAR) system, consisting of firefly luciferase under the control of a T-cell factor (TCF) response element and Renilla luciferase expressed constitutively.[45,46] For assaying the Wnt response in various HEK293 cell lines, the cells were transiently transfected with the two plasmids of the pBAR system. For all reporter assays, cells were plated in 96-well plates and grown to confluence for 24h, and then treated in duplicate for 24 h with conditioned media or the indicated purified factors, diluted in serum-free DMEM. Luminescence was measured in cell lysates with the Dual-Glo Luciferase Assay System (Promega), using a Victor3 Multilabel plate reader (Perkin-Elmer). Wnt pathway activity was calculated as the ratio of firefly to Renilla luminescence, normalized to untreated cells (incubated with serum-free DMEM), with error bars representing SD.

WNT transfer assays

To generate beads carrying NL-WNT-carrier or NL-WNT-GPC-ecto complexes, HEK293 cells stably expressing NL-WNTs were transfected with plasmids encoding HT7-tagged carriers or entire GPC ectodomains. Following transfection, the cells were switched to DMEM with 1% FBS and conditioned media were harvested every 48 h, pooled and centrifuged to remove debris. Secreted NL-WNT-carrier and NL-WNT-GPC-ecto complexes were captured on HaloLink beads (Promega), by tumbling at room temperature for 1 h. The beads were then washed extensively with TBS, after which they were used in transfer assays.

To generate beads carrying WLS-NL-WNT complexes, HEK293 cells stably expressing NL-WNTs were transfected with a plasmid encoding human WLS, C-terminally tagged with HT7. The cells were harvested and lysed in TBST supplemented with protease inhibitor cocktail (Roche). The lysate was clarified by centrifugation for 1h at 100,000g and 4°C, after which WLS-NL-WNTs were captured by tumbling with HaloLink beads for 3h at 4°C. The beads were washed extensively with wash buffer [10mM Tris-HCl, pH 7.6; 500mM NaCl, 0.5% Triton X-100 (v/v)], then with TBS with 0.02% n-dodecyl-β-D-maltoside (DDM, Anatrace).

To assay NL-WNT transfer, aliquots of the beads (5μL) were incubated with varying concentrations (1-12μM) of purified proteins diluted in HBS (20mM HEPES, pH 7.5; 150mM NaCl), with tumbling at room temperature. For transfers from WLS-NL-WNTs on beads, the acceptor proteins were diluted in HBS with 0.02% DDM. In general, WNT transfer rates were saturable at ~10μM purified acceptor. For HT7-tagged acceptor proteins, the HaloTag module was blocked by preincubation with a 20-fold excess of HaloLink-amine.[42] At different times (2, 5, 15, 30 and 60 min), aliquots of the supernatant were removed and stored on ice. At the end of the time course, NL luminescence in supernatant aliquots and on beads was measured as described above (WNT Release Assays). NL-WNT released in the supernatant was represented as percentage of the total NL signal on beads.

To generate beads carrying WLS-WNT5A, the purified complex (in 20mM HEPES, pH 7.5; 150mM NaCl; 0.1% DDM) was captured on anti-HPC antibody beads, via a C-terminal HPC peptide tag in WLS. Excess antibody was then blocked by incubation with HPC peptide. The beads were washed extensively with wash buffer [10mM Tris-HCl, pH 7.6; 500mM NaCl, 0.5% Triton X-100 (v/v)], then with TBS with 0.1% DDM. Aliquots of the beads (5μL) were incubated with purified proteins in incubation buffer (20mM HEPES, pH 7.5; 150mM NaCl; 0.1% DDM), with tumbling for 1h at room temperature. Protein in the supernatant and on beads was then analyzed by SDS-PAGE and immunoblotting.

Immunoprecipitation

Purified WNT3A-carrier complexes or carriers alone were mixed with the indicated factors in binding buffer (TBS with 2mM $CaCl_2$ and 0.2% DDM). After incubation at room temperature for 3h, the samples were subjected to immunoprecipitation with anti-HPC beads. The beads were washed three times with binding buffer. Bound proteins were eluted in elution buffer (20mM HEPES, pH 7.5; 200mM NaCl; 5mM EDTA; 100μg/mL FLAG or HPC peptide) and were analyzed by SDS-PAGE followed by immunoblotting.

Cell-based ligand binding assays

Cell-based binding assays were performed as previously described.[42] $FZD(1-10)^{KO}$ and $GPC(1-6)^{KO}$ cells were plated in poly-D-lysine–coated wells and were transfected with the indicated eGFP-tagged constructs. After 48h, cells were incubated with NL-WNT3A-SFRP2 complex or purified NL (negative control) in phenol red–free DMEM, for 1h at 37°C. Cells were then washed once with phenol red–free DMEM, fixed in 3.7% formaldehyde (m/v) in PBS, and then subjected to immunofluorescent staining using anti-NL rabbit antibodies. Nuclei were counterstained with 4',6-diamidino-2-phenylindole dihydrochloride (DAPI, Sigma-Aldrich). Images of four fields of view were acquired for each well using an automated TE2000E microscope (Nikon) equipped with an OrcaER camera (Hamamatsu) and 10× PlanApo 0.95 N.A. objective (Nikon). Images were analyzed using MATLAB as previously described.[42] Briefly, GFP images were used for cell segmentation, and background-subtracted fluorescence intensity was calculated for each cell. Bound ligand is plotted as distribution of fluorescence intensity divided by cell area, using box plots spanning from first to third quartile.

Human intestinal organoids

Human organoids from the duodenal region of the small intestine were cultured as described.[78] Briefly, organoids were derived from de-identified endoscopic biopsies collected from unaffected tissue in adolescent/young adult patients undergoing esophagogastroduodenoscopy at Boston Children's Hospital for gastrointestinal complaints. Only macroscopically normal-appearing tissue was used, from patients without a known gastrointestinal diagnosis. Informed consent and developmentally appropriate assent were obtained at Boston Children's Hospital from the donors' guardian and the donor, respectively. All methods were approved and carried out in accordance with the Institutional Review Boards of Boston Children's Hospital (Protocol number IRBP00000529). To isolate crypts, biopsies were digested with collagenase type I, agitated by pipetting, followed by centrifugation. The supernatant was removed, the crypts were resuspended in Matrigel, and 50 μL of the suspension were plated into 4–6 wells of a 48-well plate and polymerized at 37°C. Isolated crypts in Matrigel were grown in growth medium (50% v/v L-WNT3A conditioned media, 45% v/v DMEM/F12, 1% v/v Glutamax, 1% v/v N2 supplement, 1% v/v B27 supplement, 10mM HEPES, 100μg/mL primocin, 100μg normocin, 500nM A83-01, 500μM N-acetyl-cysteine, 50ng/mL recombinant murine EGF, 50nM human gastrin, 10mM nicotinamide, 10μM SB202190). Resulting organoids were passaged every 6-8 days at a 1:2 dilution, with media changes three times a week, unless otherwise specified. Importantly, these organoids are able to robustly differentiate into multiple intestinal cell types.[78] To test the effect of WNT carrier complexes, organoids were treated with ENR media (10% v/v R-spondin-1 conditioned media, 85% v/v DMEM/F12, 1% v/v Glutamax, 1% v/v N2 supplement, 1% v/v B27 supplement, 10mM HEPES, 100μg/mL primocin, 100μg/mL normocin, 500nM A83-01, 500μM N-acetyl-cysteine, 50ng/mL recombinant murine EGF, 100ng/mL Noggin, 50nM human gastrin, 10mM nicotinamide, 10μM SB202190), with or without fresh conditioned media from L-WNT3A cells, concentration-adjusted commercial WNT3A (R&D Systems), or purified WNT-carrier complexes in 20mMHEPES, pH 7.5; 150mM NaCl. Representative light microscopy images of organoids were taken at 2x magnification using an Invitrogen EVOS FL 2 Auto microscope. The numbers and viability of organoids were analyzed manually or by luminescence cell viability assay using CellTiter Glo-3D (Promega) at every passage.

Please cite this article in press as: de Almeida Magalhaes et al., Extracellular carriers control lipid-dependent secretion, delivery, and activity of WNT morphogens, Developmental Cell (2023), https://doi.org/10.1016/j.devcel.2023.11.027

QUANTIFICATION AND STATISTICAL ANALYSIS

Statistical parameters for experiments involving quantitative comparisons are reported in the figure legends. Where indicated, measures of Wnt pathway activation were normalized to an untreated control, as described. All qualitative experiments (e.g. WNT release experiments, NL-WNT transfer experiments and immunoprecipitation) were performed at least twice on separate days and, where possible, with different preparations of the reagents involved. For imaging-based assays, the number of cells used to calculate median fluorescence intensity values is indicated in the figure legends. For organoid cell viability assay, data were analyzed by one-way ANOVA with Tukey's post-tests. $P < 0.05$ was considered significant.